Geochemistry of back arc basin volcanism in Bransfield Strait, Antarctica: Subducted contributions and along-axis variations

Randall A. Keller,[1] Martin R. Fisk,[1] John L. Smellie,[2] Jorge A. Strelin,[3]
Lawrence A. Lawver,[4] and William M. White[5]

Received 13 February 2001; revised 15 October 2001; accepted 25 October 2001; published 23 August 2002.

[1] Bransfield Strait is a Quaternary, ensialic back arc basin at the transition from rifting to spreading. Fresh volcanic rocks occur on numerous submarine features distributed along the rift axis, including a discontinuous neovolcanic ridge similar to the nascent spreading centers seen in some other back arc basins. Smaller edifices near the northeast end of the rift yielded basalts with the most arc-like compositions (e.g., high large-ion lithophile element/high field strength element and $^{87}Sr/^{86}Sr$). The most mid-ocean ridge basalt (MORB)-like basalts are from a large, caldera-topped seamount and a 30-km-long axial neovolcanic ridge toward the southwest end of the rift, but these two features also yielded andesite and rhyolite, respectively. The volcanic and geochemical variations are not systematic along axis and do not reflect the unidirectional propagation of rifting suggested by geophysical data. The most depleted basalts have major and trace element characteristics indistinguishable from MORB except for slightly higher Cs and Pb concentrations. Pb isotopic ratios show little variation compared to Sr and Nd isotopic ratios and do not extend to the depleted Pb isotopic ratios found in other back arc basins. Either the depleted mantle beneath Bransfield Strait has higher than normal Pb isotopic ratios or the subducted component beneath Bransfield Strait has such high Pb concentrations that it dominates the Pb isotopic composition of the Bransfield Strait mantle without significantly affecting the Sr and Nd isotopic compositions. Metalliferous sediments and fluids extracted from a subducting slab may have the necessary high concentrations of Pb. *INDEX TERMS:* 1040 Geochemistry: Isotopic composition/chemistry; 3640 Mineralogy and Petrology: Igneous petrology; 3655 Mineralogy and Petrology: Major element composition; 3670 Mineralogy and Petrology: Minor and trace element composition; *KEYWORDS:* back arc basin, Bransfield Strait, Antarctica, geochemistry, volcanism, recycling

1. Introduction

[2] Studies of the back arc basins (BABs) in the western Pacific produced a generalized model for back arc basin formation wherein oceanic island arc crust is rifted into a series of subbasins that are then taken over by a propagating seafloor spreading center [e.g., *Tamaki et al.*, 1992; *Hawkins*, 1995]. Little is known, however, about how BABs form in continental crust, perhaps because ensialic BABs are rare (Bransfield Strait and Okinawa Trough may be the only active ensialic BABs that are opening without a large strike-slip component). A propagating rift model has also been proposed for Bransfield Strait [*Barker and Austin*, 1998] based upon seismic surveys that reveal extensive volcanic basement at the northeast end of the rift and more isolated volcanic features at the southeast end of the rift. We undertook a geochemical study of the rift-related volcanism to determine if there are along-axis variations in the lava chemistry that coincide with the geophysical evidence for a propagating rift model.

[3] The composition of basalts erupted in BABs (BABBs) can range from those resembling basalts created by melting of the depleted upper mantle at a mid-ocean ridge (mid-ocean ridge basalt (MORB)-like) to those resembling basalts created by the interaction of subducted lithosphere with the mantle wedge at a subduction zone (arc-like) [e.g., *Saunders and Tarney*, 1984]. MORB-like basalt dominates in the more mature (spreading) BABs, but it can also occur very early in the history of a BAB, and arc-like volcanism can occur at any time [*Taylor and Karner*, 1983; *Hochstaedter et al.*, 1990; *Keller et al.*, 1992]. It is still debatable whether the dominance of MORB-like basalts later in the development of a BAB is caused by increasing influx of depleted mantle as the BAB develops or whether it is simply an aftereffect of preferential melting and removal of enriched portions of the mantle during the early stages of rifting [*Hawkins*, 1995]. Bransfield Strait is a back arc rift which, based upon comparison to other BABs, appears to be at the transition from rifting to spreading. This

[1] College of Oceanic and Atmospheric Sciences, Oregon State University, Corvallis, Oregon, USA.
[2] British Antarctic Survey, Cambridge, UK.
[3] Instituto Antartico Argentino, Buenos Aires, Argentina.
[4] Institute for Geophysics, University of Texas at Austin, Austin, Texas.
[5] Department of Earth and Atmospheric Sciences, Cornell University, Ithaca, New York.

0148-0227/02/2001JB000444$09.00

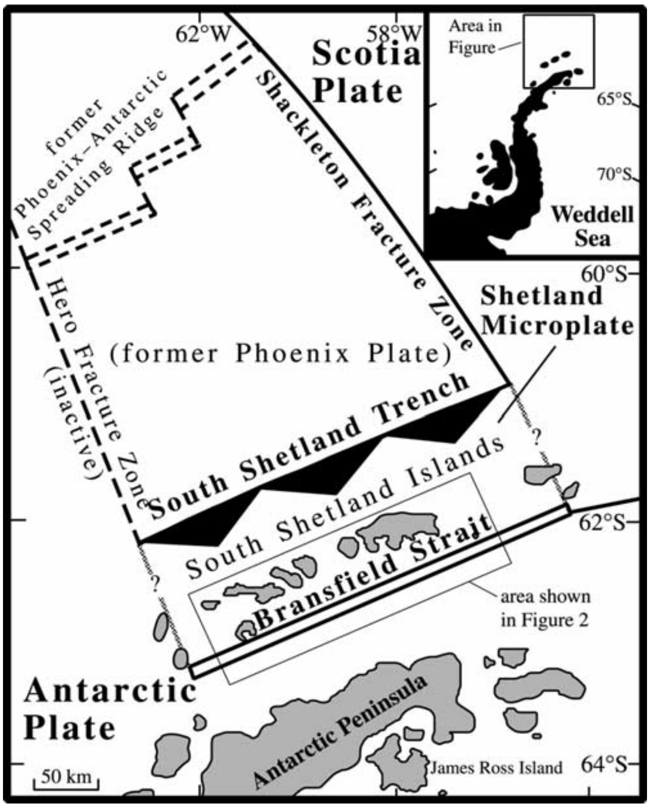

Figure 1. Generalized tectonic map of the northern Antarctic Peninsula (area shown in inset). The South Shetland Trench (shown by black triangles pointing to the overriding plate), the rift in the Bransfield Strait, and the Shackleton Fracture Zone are still active, but the Phoenix-Antarctic Ridge ceased spreading <4 Myr ago [*Maldonado et al*., 1994; *Maldonado and Livermore*, 1999]. The rectangle around part of the Bransfield Strait and South Shetland Islands shows the area covered by the bathymetric map in Figure 2.

makes it an excellent place to study how a magmatic system makes the transition from arc-like to MORB-like volcanism.

2. Background

[4] At the northern tip of the Antarctic Peninsula, the former Phoenix Plate (now part of the Antarctic Plate) is subducting to the southeast into the South Shetland Trench (Figure 1) [*Barker*, 1982; *Maldonado et al.*, 1994]. The Antarctic Peninsula magmatic arc associated with this subduction was most recently active in the Early Miocene on what are now the South Shetland Islands [*Smellie et al.*, 1984]. Evidence for continuing subduction includes ongoing deformation of the trench sediments [*Maldonado et al.*, 1994] and earthquakes as deep as 55 km [*Pelayo and Wiens*, 1989].

[5] Behind the South Shetland Islands arc, rifting in the Bransfield Strait caused thinning of the 40-km-thick continental arc crust. Under the Bransfield Strait, normal mantle velocities are observed below about 30 km, but anomalously fast crustal velocities (or anomalously slow mantle velocities?) of 7–8 km/s are observed at depths of <10 km [*Grad et al.*, 1993, 1999].

[6] Quaternary volcanism associated with the rifting in Bransfield Strait ranges from basaltic andesite similar to island arc tholeiite to tholeiite similar to MORB to one volcanic island with a basalt-to-trachydacite evolutionary suite [*Weaver et al.*, 1979; *Keller et al.*, 1992]. Two volcanoes on the northern margin of the strait (Melville Peak and Penguin Island, Figure 2) and two volcanoes near the rift axis (Bridgeman Island and Deception Island) are above the sea surface and have been studied in detail [*Weaver et al.*, 1979; *Birkenmajer*, 1980; *Birkenmajer and Keller*, 1990; *Birkenmajer*, 1992; *Keller et al.*, 1992; *Smellie et al.*, 1992; *Marti et al.*, 1996; *Smellie*, 2001]. However, the focus of this paper is the submerged volcanoes which constitute most of the volcanism in the rift and form isolated seamounts and a discontinuous axial neovolcanic ridge roughly aligned with Deception and Bridgeman Islands (Figure 2) [*Fisk*, 1990; *Keller and Fisk*, 1992; *Keller et al.*, 1992; *Lawver et al.*, 1995, 1996]. The axial ridge is similar to the nascent seafloor spreading center in the Mariana Trough [*Hawkins et al.*, 1990], suggesting that Bransfield Strait may be just progressing beyond the rifting stage and into the earliest stages of seafloor spreading [*Gracia et al.*, 1996].

[7] A prominent magnetic high along the axis of the strait coincides with the discontinuous neovolcanic ridge, but evidence for seafloor spreading in the magnetic anomalies is contentious. P. J. Roach (as cited by *Barker and Dalziel* [1983]) and *González-Ferrán* [1991] report that models with reversely magnetized crust at the edges of the rift basin best fit the data, suggesting that almost the entire floor of the basin is underlain by oceanic crust created by 1.3–2 Myr of seafloor spreading. However, seismic refraction data show that the crust is too thick to be normal oceanic crust [*Grad et al.*, 1993], and seismic reflection and bathymetric data show multiple locations of recent extension and volcanism [*Klepeis and Lawver*, 1994; *Barker and Austin*, 1994, 1998]. This argues against a history of seafloor spreading, and the uncertain magnetic characteristics of the thick sediment cover with interbedded basalt flows [*Lawver and Hawkins*, 1978] and the difficulty of unambiguously modeling such short magnetic profiles led *Lawver et al.* [1995] to question the application of the seafloor spreading model to the Bransfield Strait magnetic data. Thus, if rifting has progressed to focused spreading in the strait as suggested by the prominent neovolcanic ridge, this transition must be ongoing or very recent.

[8] Some BABs have systematic along-axis variations in rift morphology, grading from a diffuse rift to a focused spreading center (e.g., Gulf of California [*Saunders*, 1983] and Lau Basin [*Hawkins*, 1995]). The Bransfield rift does not have a well-developed spreading center, but the morphology of some of the Bransfield features has been interpreted as a developmental progression from seamount volcanism (the seamount at 58.4°W) to a rifted seamount with a central ridge (the lineated feature at 59.8°W) to a long ridge flanked by rifted seamount remnants (the ridge at 59.0°W) [*Gracia et al.*, 1996]. The best developed feature is located between two less developed features, however, so if there is a progression in rift morphology in Bransfield Strait, it is not systematic from one end of the rift to the other.

[9] Prior to this work only two closely spaced seamounts had been dredged in Bransfield Strait (ES and WS in Figure 2

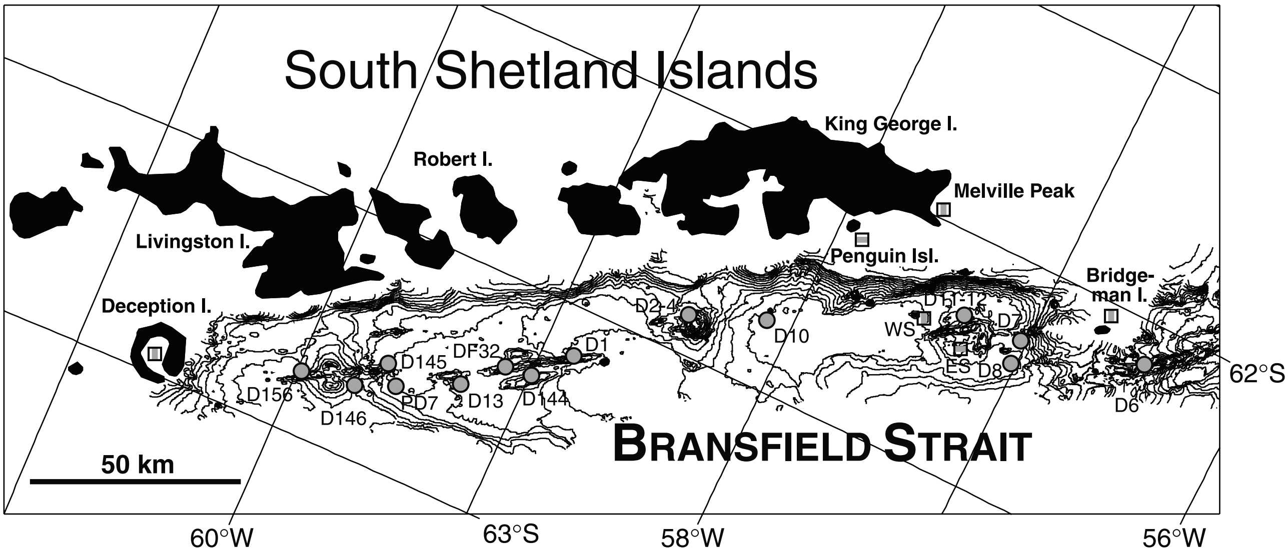

Figure 2. Bathymetric map of Bransfield Strait [after *Lawver et al.*, 1996] with 100-m contour interval. Sampled locations of Quaternary volcanism are shown by symbols. Squares are island and dredge sample locations from *Fisk* [1990], *Keller and Fisk* [1992], and *Keller et al.* [1992] (ES, Eastern Seamount, and WS, Western Seamount). Circles are locations of new data. DF32 and PD7 are piston-cored samples DF86.32 and PD89.4.7, respectively. Other circles are dredged samples.

[*Keller and Fisk*, 1989]). These rocks are compositionally transitional between island arc basalts and mid-ocean ridge basalts (MORB), and thus similar to some back arc basin basalts (BABBs) [*Fisk*, 1990; *Keller and Fisk*, 1992]. Since that study we have undertaken a more thorough sampling of the submarine volcanism to determine the amount of along-axis variation in this young ensialic marginal basin. Bathymetric maps [*Klepeis and Lawver*, 1994; *Gracia et al.*, 1996; *Lawver et al.*, 1996] revealed the highly lineated nature of the steep-sided ridges between Deception and Bridgeman Islands, including at least a dozen features that could be volcanic (Figure 2).

3. Sample Locations and Descriptions

[10] In February-March 1993, cruise NBP93-1 of the RVIB *Nathaniel B. Palmer* recovered fresh volcanic rocks in eight dredges (D1–D10) in Bransfield Strait from some of the newly mapped features [*Keller et al.*, 1994]. All but one of the dredges also contained rounded erratics ice-rafted from the South Shetland Islands and the Antarctic Peninsula. At about the same time, the British Antarctic Survey (BAS) ship RRS *James Clark Ross* also recovered fresh volcanic rocks in four dredges (D144–D156) in Bransfield Strait. In November 1995, cruise NBP95-7 of the RVIB Nathaniel B. Palmer recovered fresh volcanic rocks in three more dredges (D11–D13) in Bransfield Strait [*Lawver et al.*, 1996]. Samples from all three cruises were carefully examined for weathered or rounded surfaces, and only those that appeared to be fresh and unequivocally derived in situ from outcrops were selected for further analyses.

[11] The new samples, from southwest to northeast, are (circles in Figure 2): dredges D145, D146, D156, and piston core PD89.4.7 (PD7 in figures and tables) from a shallow elongate feature with a central ridge centered at 59.8°W just northeast of Deception Island; dredge D13 from a small volcano at 59.4°W that is aligned with the main neovolcanic ridges; piston core DF86.32 (DF32 in figures and tables [*Anderson et al.*, 1987]) and dredges D1 and D144 from a 30-km-long, axial ridge centered at 59.0°W; dredges D2, D3, and D4 from a large, caldera-topped seamount at 58.4°W; dredge D10 from a small seamount at 58.1°W; dredges D11 and D12 from the hook-shaped ridge centered at 57.3°W; dredge D8 from a short, steep-sided linear feature at 57.1°W; dredge D7 from the southwest tip of a linear ridge coming off of the Bridgeman Island platform; and dredge D6 from a small seamount just east of Bridgeman Island at 56.6°W. Also shown in Figure 2 (as squares) are the locations of previously analyzed submarine and subaerial samples in Bransfield Strait [see *Keller and Fisk*, 1989; *Fisk*, 1990; *Keller and Fisk*, 1992; *Keller et al.*, 1992].

[12] Rubbly chunks of pillows and flows were the most common form of sample recovered. Most samples have at least one glassy surface and contain abundant vesicles. Dredges D11, D12, D13, and D144 included cryptocrystalline to glassy black rhyolite. Higher proportions of the basalts in dredges D1, D2, and D8 had fresh glass, but fresh to only slightly palagonitized glass could be found in every dredge except D4 and D7, in which the glass was all slightly to moderately palagonitized. The lack of fresh glass in a dredge may not be a reliable measure of the age of the feature; for example, D4 contained little fresh glass, while D2 from the same volcano contained a high proportion of fresh glass. Other than slight to moderate palagonitization in many of the samples, no alteration minerals or zeolitization were observed.

[13] In hand sample, many of the basalts are virtually-to-completely aphyric. A few samples from D1–D4 contain trace amounts of plagioclase microlites, while a few samples from D8 contain rare olivine microphenocrysts, and most samples from D6 contain a few percent olivine and plagioclase microphenocrysts. The only truly porphyritic samples are from D10, which contain up to 15% olivine,

Table 1. Representative Electron Microprobe Analyses of Bransfield Strait Glass Samples[a]

Sample	SiO_2	TiO_2	Al_2O_3	FeO*	MnO	MgO	CaO	Na_2O	K_2O	P_2O_5	Sum
D1A	57.56	1.49	15.08	9.52	0.22	3.70	6.85	4.50	0.51	0.31	99.74
D1B	55.14	1.46	15.17	9.39	0.20	4.47	8.26	4.29	0.40	0.30	99.08
D1F	53.99	1.81	14.82	10.12	0.17	4.58	8.84	4.09	0.38	0.29	99.09
D1I	55.84	1.34	15.46	8.84	0.17	4.48	8.27	4.51	0.43	0.27	99.61
D1J	54.21	1.89	14.76	10.43	0.13	4.16	8.15	4.15	0.43	0.33	98.64
D1N	52.24	1.82	15.02	10.45	0.19	5.35	9.63	3.74	0.23	0.20	98.87
D2A	53.47	2.20	14.24	11.88	0.17	4.13	8.19	4.29	0.44	0.31	99.31
D2B	56.39	2.18	14.81	11.29	0.17	3.21	6.56	4.29	0.60	0.43	99.93
D2E	54.46	2.28	13.67	12.36	0.16	3.72	6.96	4.16	0.54	0.39	98.70
D2G	49.63	1.33	16.50	9.01	0.10	7.58	11.66	3.03	0.15	0.13	99.13
D2J	59.92	1.67	15.07	9.44	0.21	2.15	5.16	4.59	0.76	0.47	99.44
D3C	51.12	1.54	14.78	9.68	0.11	5.86	10.46	3.58	0.28	0.18	97.59
D3D	52.12	2.72	13.56	13.04	0.20	3.71	7.90	4.03	0.43	0.35	98.07
D4D	52.40	2.13	13.93	11.77	0.19	4.89	8.99	4.02	0.37	0.24	98.92
D4F	53.78	2.78	13.64	12.79	0.17	3.87	7.68	3.97	0.50	0.35	99.53
D6D	51.82	0.84	16.08	8.45	0.12	7.12	12.00	2.55	0.39	0.06	99.42
D7B	54.76	1.36	14.69	10.44	0.16	4.58	8.92	3.55	0.57	0.12	99.14
D7E	53.79	1.09	15.36	9.54	0.16	5.07	9.59	3.40	0.53	0.10	98.61
D7F	54.95	0.85	15.38	8.68	0.11	5.45	10.00	3.11	0.52	0.10	99.14
D7H	53.28	1.29	14.73	10.32	0.16	4.45	8.81	3.52	0.57	0.13	97.26
D7O	52.71	1.00	15.28	8.84	0.16	5.58	10.41	3.17	0.45	0.09	97.68
D8F	50.52	1.23	16.45	8.15	0.14	6.73	10.98	3.01	0.32	0.13	97.66
D10A	51.20	1.14	15.59	7.95	0.10	6.62	11.80	2.74	0.63	0.29	98.06
D10J	52.13	1.09	15.85	8.32	0.12	6.14	11.48	2.91	0.67	0.24	98.95
D11.2	76.19	0.39	12.06	4.79	0.11	0.15	1.79	3.52	1.22	0.10	100.67
D11.3	78.05	0.34	11.01	4.27	0.11	0.11	1.02	3.04	1.06	0.06	99.53
D12.3	78.63	0.30	11.27	4.12	0.11	0.12	1.22	3.02	1.37	0.08	100.58
D13.1	54.41	1.74	15.86	7.81	0.14	3.67	9.31	4.65	0.55	0.35	98.57
D13.4	75.14	0.49	11.80	5.76	0.16	0.19	1.75	2.95	1.16	0.07	99.94
PC7	54.80	1.85	15.59	9.76	0.15	4.21	8.08	4.63	0.52	0.28	99.86
DF32	54.79	2.18	14.20	10.78	0.20	4.40	8.07	3.99	0.43	0.33	99.37

[a] Analyzed at Oregon State University. See Appendix A for details.

and a few samples from D7, which contain up to 5% plagioclase + clinopyroxene + olivine. The samples are unusually vesicular for basalts dredged from these depths (700–1950 m [*Keller et al.*, 1994]). A few of the samples in dredges D1, D2, and D7 contain <10% vesicles, but otherwise all samples contain 10–40% vesicles.

[14] In thin section, most of the samples contain rare microphenocrysts of plagioclase ± olivine ± clinopyroxene in a groundmass of plagioclase microlites + glassy mesostasis ± olivine ± clinopyroxene. The exceptions are D6 and D7, which contain a few percent plagioclase ± clinopyroxene ± olivine in a groundmass similar to the aphyric sections, and D10, which contains 15% olivine in a glassy groundmass.

4. Results

[15] Major elements in glasses were determined by electron microprobe. A representative subset of those samples plus 10 samples for which no glass was available (i.e., dredges D144–D146 and D156 and five representative South Shetland Island Arc samples) were analyzed for major and trace elements by XRF. Additional trace elements were determined by inductively coupled plasma–mass spectrometry (ICP-MS) on the same subset of samples. Sr, Nd, and Pb isotopic analyses were performed on a smaller subset of samples dredged from BS and the five samples from the South Shetland arc. See Appendix A for the analytical techniques.

4.1. Major Elements

[16] We analyzed clean glass chips from 87 samples from dredges D1–D4, D6–D8, and D10–D13 and the two piston cores (DF86.32 and PD89.4.7) for major elements by electron microprobe (Table 1; see Appendix A). The samples are subalkaline basalts and basaltic andesites, except for two andesites and four rhyolites. The basalts are all olivine tholeiites with the exceptions of D144.4 and D156.4, which contain trace amounts of normative nepheline and could be considered alkalic basalts. MgO concentrations in the glasses range from 0.1 wt % (D12.3) to 8.1 wt % (D2H). Every major element except CaO has a significant range of concentrations at a given MgO (Figure 3), so the samples cannot all be related by a single liquid line of descent.

[17] All of the major elements except Al_2O_3 and CaO increase with decreasing MgO across almost the entire sample suite (excluding the rhyolites). Al_2O_3 and CaO decrease with decreasing MgO, suggesting that plagioclase and possibly pyroxene were fractionating across the whole suite of rocks. The rhyolites (D11.2, D11.3, D12.3, and D13.4) have the lowest concentrations of all of the major elements (except SiO_2 and K_2O) and are obviously extensively fractionated; even their Na_2O and P_2O_5 concentrations are low (Table 1).

[18] Samples from D2–D4 (all from the large seamount at 58.4°W) have high TiO_2, FeO*, and Na_2O and lower K_2O at a given MgO, while D6, D7, D10, and D13 (all from small seamounts) have low TiO_2 and FeO*. D6 and D7 are notable for their low TiO_2 and P_2O_5 and high Al_2O_3 and CaO. D1 and the two piston-cored samples (DF32 and PD7) are our only glass analyses from the southwestern end of the rift, and they, like D2–D4, have high Na_2O and low K_2O but do not have the high FeO* and TiO_2 found in D2–D4.

[19] The chemical differences between the glasses are more obvious when they are plotted by element ratios that

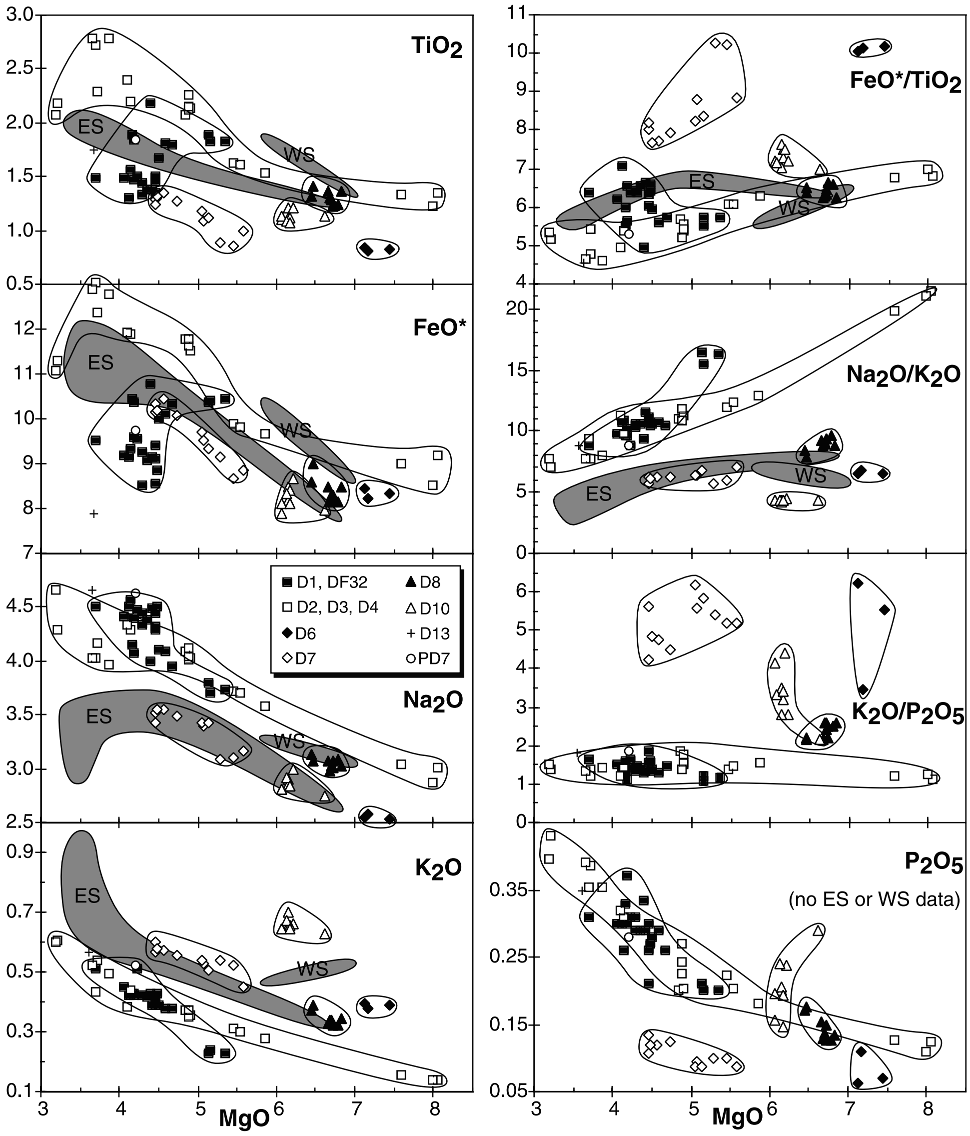

Figure 3. Major element plots of Bransfield Strait glass analyses determined by electron microprobe (locations in Figure 2). WS and ES fields are published data for Western Seamount and Eastern Seamount in Bransfield Strait [*Fisk*, 1990]. Values are in wt %.

are insensitive to fractionation of basaltic minerals (Figure 3). The high Na_2O and low K_2O of D1–D4 give them a much higher Na_2O/K_2O than the other dredges. K_2O/P_2O_5 values are also obviously lower in D1–D4. FeO^*/TiO_2 is less definitive, though significantly higher in D6 and D7 than the other dredges, with D10 being perhaps transitional. The two piston-cored samples fall in the same area as D1–D4 on all of the plots.

[20] Whole rock major element compositions (Table 2) grossly resemble the glass compositions, with the notable exception that olivine accumulation in the basalts causes MgO to be as much as 11 wt % higher in the whole rocks (Figure 4), but we include both glass and whole rock figures and data here because we do not have glass data for dredges D144–D156 and from the islands. Sample locations that group together in their glass chemistry are also similar in whole rock chemistry, e.g., the high Na_2O/K_2O and low K_2O/P_2O_5 of the D1–D4 glass data are also obvious in the whole rock data.

[21] Dredges D144–D156 have high Na_2O and low K_2O (Figure 4), similar to other samples from the southwest end of the rift (i.e., D1–D4 and the piston-cored samples). The rhyolite from D144 has low P_2O_5 and must have experienced apatite fractionation; however, it is not included in these plots to maintain a reasonable scale. For comparison, the subaerial Bransfield Strait volcanoes [*Weaver et al.*, 1979; *Keller et al.*, 1992] have as wide a range of compositions as the dredged samples (Figure 4). Bridgeman Island has high Al_2O_3, FeO^*/TiO_2, and K_2O/P_2O_5, similar to the nearby dredges D6 and D7. Penguin Island and Melville Peak are on the northern margin of the rift basin and do not consistently resemble any of the dredged samples, although they do both have low Na_2O/K_2O like other locations on the northeast end of the rift. Also the basalt-to-trachydacite suite on Deception Island (only samples with >4 wt % MgO are shown in Figure 4) has high Na_2O like other samples from the southwest end of the rift. This high-Na_2O and low-K_2O nature of the samples from the southwest part of the rift

Table 2. Representative XRF Analyses of Whole Rock Samples From Bransfield Strait and the South Shetland Islands[a]

	SiO_2	TiO_2	Al_2O_3	FeO*	MnO	MgO	CaO	Na_2O	K_2O	P_2O_5	LOI	Total	V	Cr	Ni	Cu	Zn	Ga
D1A	54.05	1.45	15.57	8.73	0.18	4.52	8.40	4.77	0.40	0.24	0.28	98.59	189	43	23	49	85	20
D1F	52.91	1.72	15.62	9.50	0.18	5.27	9.12	4.17	0.41	0.23	−0.10	99.03	244	35	16	46	85	19
D2G	49.04	1.37	17.03	8.77	0.16	7.61	11.61	3.08	0.18	0.11	−0.26	98.70	212	219	61	69	68	16
D2N	52.15	2.75	14.80	11.94	0.22	3.93	7.83	5.04	0.39	0.34	−0.31	99.08	340	3	8	37	109	22
D3C	51.14	1.56	16.23	9.31	0.17	6.03	10.87	3.54	0.27	0.14	−0.25	99.01	272	49	32	70	76	20
D4D	51.91	1.95	15.66	10.54	0.19	4.80	9.23	4.37	0.32	0.20	−0.38	98.79	344	6	15	70	92	22
D6D	50.11	0.69	15.79	8.09	0.14	11.21	10.60	2.22	0.31	0.03	−0.13	99.06	221	631	235	65	63	17
D7A	51.51	0.69	18.07	6.90	0.12	7.33	11.95	2.52	0.32	0.04	0.04	99.49	195	174	63	68	54	17
D7F	52.63	0.65	18.37	6.78	0.13	5.82	11.49	2.83	0.38	0.05	0.19	99.32	209	56	33	67	59	17
D8F	50.81	1.18	16.14	8.58	0.16	8.84	10.19	2.88	0.40	0.10	0.10	99.38	267	462	187	63	71	19
D10A	48.29	0.75	12.70	8.56	0.15	17.57	8.58	1.99	0.41	0.10	−0.04	99.06	238	1073	608	71	67	14
D144.1	70.28	0.35	12.89	4.45	0.13	0.12	1.26	7.39	1.42	0.01	1.17	99.47	10	5	6	13	125	29
D144.4	50.06	1.47	17.08	8.69	0.16	6.40	10.71	3.83	0.32	0.17	0.23	99.12	269	129	54	64	75	19
D145.3	51.50	1.39	17.00	8.50	0.16	5.85	10.61	3.91	0.37	0.16	0.12	99.57	249	37	33	80	71	19
D146.1	50.97	1.57	17.38	8.37	0.16	5.94	10.42	3.88	0.32	0.18	−0.20	98.99	218	114	52	58	72	17
D156.4	50.02	1.50	17.59	8.21	0.15	6.34	11.12	3.68	0.34	0.20	−0.20	98.95	225	147	44	66	64	20
P615.1	47.97	0.51	20.06	7.66	0.13	6.82	12.70	2.04	0.58	0.11	0.95	98.58	212	79	37	95	56	18
P842.9	50.30	1.10	16.50	2.31	0.17	8.90	10.48	2.56	0.54	0.48		93.34		200	67			
P864.4	49.86	1.02	16.91	9.66	0.17	6.47	11.65	2.45	0.23	0.14	0.14	98.56	299	113	40	72	70	16
P845.9	46.57	1.33	19.70	10.82	0.17	5.09	11.47	2.59	0.30	0.17	0.34	98.21	364	30	13	56	74	21
P862.4	47.97	0.76	22.10	9.04	0.16	3.55	12.46	2.32	0.51	0.11	0.26	98.98	273	18	14	62	57	19

[a] Analyzed at NERC, UK, using procedures given by *Smellie et al.* [1995]. FeO* is total Fe as FeO. The South Shetland Islands samples are P615.1 from King George Island; P842.9 from Robert Island; and P864.4, P845.9, and P862.4 from Livingston Island. See *Smellie et al.* [1984] for sample locations.

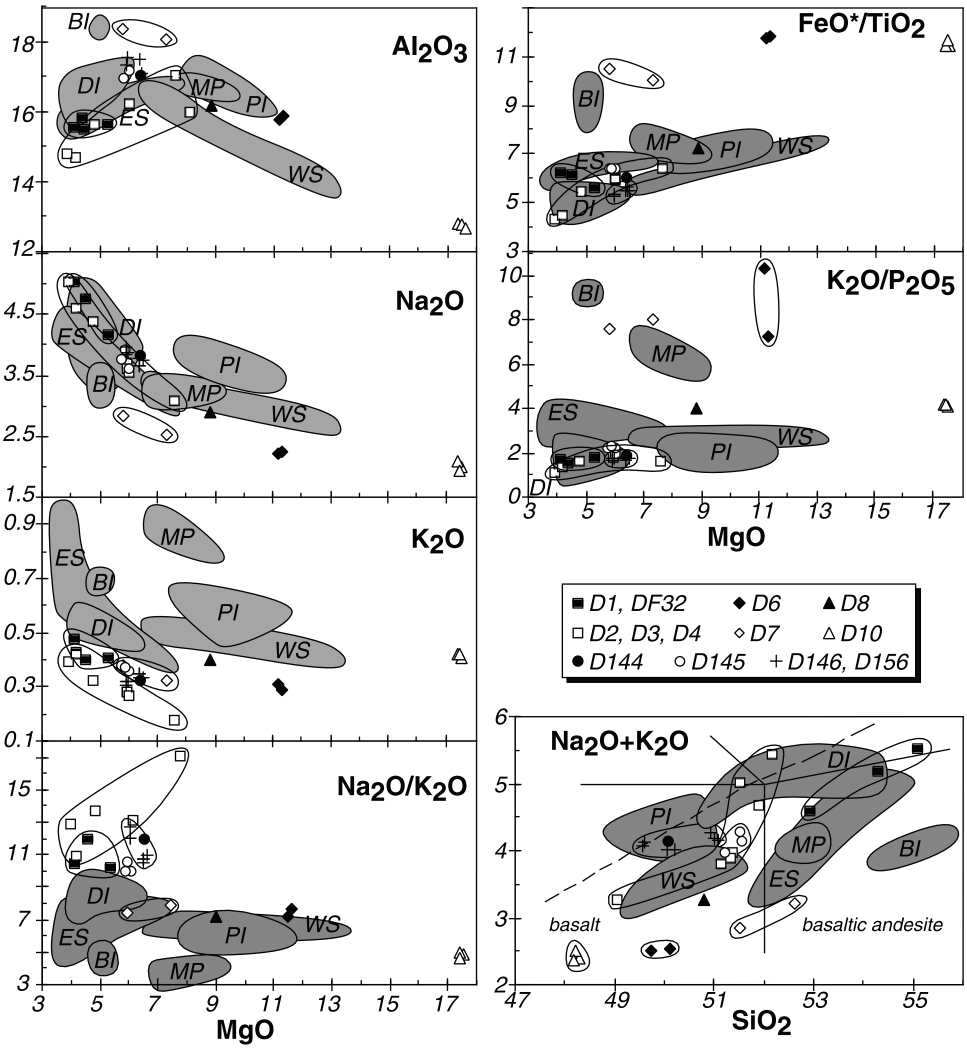

Figure 4. Major element plots of Bransfield Strait whole rock lavas. Shaded fields are published data [from *Keller and Fisk*, 1992; *Keller et al.*, 1992] for other Bransfield Strait locations (abbreviations as in Figure 3; also BI, Bridgeman Island; DI, Deception Island; MP, Melville Peak; and PI, Penguin Island). Values are in wt %.

therefore appears to be a regional feature: all locations west of 58°20'W, both subaerial and submarine, in Bransfield Strait have this relatively high Na_2O/K_2O.

4.2. Trace Elements

[22] Incompatible trace element concentrations are reported in Tables 2 and 3 and shown in Figure 5. At any given MgO, there is a range of trace element concentrations, which is again far too great to be explained by simple fractional crystallization. Elements that are abundant and highly mobile in subduction zone magmas, such as Rb and Ba, show more variation than elements with higher field strengths, such as Zr and Nb (Figure 5). This is especially true when data from the earlier dredges (ES and WS in figures) and the Bransfield Strait subaerial samples are included in the comparison. Also, although there is some overlap, samples from the southwest end of the rift (D1–D4, D144–156, piston cores, and Deception Island) tend to have lower Ba and Rb and higher Y, Zr, and Nb, making them less arc-like than samples from the northeast end of the rift.

[23] If we assume that MORB values give an indication of what partial melting of the depleted upper mantle produces when it is unaffected by subduction zone processes [*Pearce and Parkinson*, 1993], we can readily determine how subduction has affected the magma sources and processes at the South Shetland Islands and Bransfield Strait by comparing our samples to MORB. By plotting the trace element data on a MORB-normalized multielement plot (Figure 6), it is readily apparent which elements are high (''enriched'') and low (''depleted'') relative to MORB. To characterize the subduction-related volcanism in this region, we analyzed five representative South Shetland Arc basalts from a range of locations and time periods (123–51 Ma; Tables 2, 3, and 4 and Figure 6a) and include data from a 24 Ma arc basalt from King George Island [*Keller et al.*, 1992]. Compared to normal MORB (NMORB), or even enriched MORB (EMORB in Figure 6a), the arc volcanism has high Cs, Ba, Th, U, K, Pb, and Sr (although Cs has been disturbed by alteration in some of the arc rocks) and low Nb, Ta, and possibly Zr and Hf. These

Table 3. Representative ICP-MS Whole Rock Analyses of Bransfield Strait and South Shetland Islands Samples

	Rb	Sr	Y	Zr	Nb	Cs	Ba	La	Ce	Pr	Nd	Sm	Eu	Gd	Tb	Dy	Ho	Er	Tm	Yb	Lu	Hf	Ta	Pb	Th	U
D1A	3.5	174	60	272	6.0	0.27	38	9.52	29.48	4.83	22.98	6.94	2.03	7.87	1.45	9.28	2.02	5.99	0.92	5.66	0.86	6.75	0.45	2.17	0.56	0.31
D1F	3.3	192	47	207	5.1	0.24	35	7.92	23.85	3.95	18.53	5.62	1.76	6.47	1.18	7.53	1.62	4.82	0.74	4.54	0.70	5.09	0.36	2.08	0.51	0.24
D1J	4.1	199	53	235	5.9	0.23	38	8.95	26.34	4.22	21.11	6.47	1.98	7.45	1.34	8.34	1.78	5.18	0.78	5.06	0.80	5.56	0.43	1.87	0.53	0.27
D1N	3.6	220	36	142	3.2	0.12	29	5.35	15.75	2.61	13.31	4.18	1.49	5.16	0.92	5.93	1.27	3.64	0.55	3.50	0.56	3.47	0.25	1.32	0.27	0.17
D2G	1.6	204	30	106	2.4	0.09	20	4.02	12.17	2.22	10.81	3.44	1.30	3.92	0.74	4.67	1.02	2.90	0.47	2.71	0.40	2.60	0.19	0.95	0.22	0.13
D2J	8.6	163	82	407	10.9	0.46	95	16.57	46.61	7.24	35.77	10.13	2.96	12.11	2.15	12.97	2.93	8.24	1.25	8.01	1.25	9.65	0.79	4.62	1.34	0.63
D2N	4.2	213	55	226	7.0	0.28	58	9.39	28.07	4.75	22.59	6.65	2.32	7.71	1.38	8.81	1.90	5.46	0.86	5.14	0.77	5.38	0.52	2.30	0.64	0.33
D3C	3.2	219	34	127	3.6	0.18	39	5.23	15.14	2.47	12.76	4.02	1.50	4.93	0.89	5.57	1.20	3.42	0.49	3.24	0.48	3.10	0.26	1.74	0.39	0.24
D4D	3.6	219	44	175	4.8	0.22	47	7.06	20.00	3.35	16.81	5.06	1.78	6.23	1.11	6.90	1.52	4.39	0.64	4.15	0.66	4.22	0.34	2.04	0.50	0.25
D6D	7.4	193	15	40	0.7	0.46	53	2.45	6.17	1.05	5.09	1.68	0.63	1.95	0.37	2.40	0.53	1.54	0.24	1.48	0.22	1.22	0.07	2.29	0.57	0.24
D6G	12.2	380	12	42	0.6	0.53	79	2.77	6.88	1.06	5.07	1.60	0.66	1.93	0.32	1.94	0.40	1.16	0.17	1.10	0.18	1.26	0.04	3.14	0.74	0.34
D7A	5.5	277	16	48	0.7	0.29	44	2.50	6.73	1.17	5.66	1.89	0.74	2.18	0.39	2.53	0.55	1.61	0.25	1.47	0.23	1.49	0.07	1.93	0.51	0.21
D7F	8.2	237	17	58	1.0	0.48	67	3.32	8.45	1.38	6.45	1.91	0.73	2.33	0.42	2.71	0.59	1.76	0.27	1.75	0.24	1.66	0.08	2.40	0.79	0.30
D8F	7.2	190	25	82	1.5	0.38	57	3.92	11.21	1.91	9.23	2.90	1.07	3.35	0.61	3.93	0.86	2.53	0.39	2.39	0.34	2.20	0.11	2.27	0.58	0.41
D10A	10	223	15	61	1.6	0.34	138	6.67	15.68	2.24	9.20	2.29	0.78	2.43	0.41	2.55	0.53	1.57	0.23	1.46	0.22	1.70	0.13	2.84	1.59	0.41
D144.1*	15	22	153	998	18.0	1.20	125	28.00	80.00	12.00	57.00	16.00	2.30	18.00	3.50	22.00	5.00	16.00	2.50	16.00	2.60	23.00	1.30	7.10	2.60	1.10
D144.4	4.6	297	31	124	3.7	0.24	71	5.81	16.05	2.51	12.84	3.75	1.35	4.51	0.82	5.17	1.11	3.11	0.46	2.93	0.46	3.10	0.26	2.99	0.52	0.21
D145.3	2.9	352	25	112	4.0	0.26	66	6.53	16.74	2.54	12.55	3.51	1.23	3.85	0.71	4.20	0.89	2.49	0.38	2.34	0.36	2.67	0.27	2.32	0.51	0.20
D146.1	2.2	324	30	130	3.6	0.10	46	6.59	17.63	2.76	13.65	4.06	1.49	4.74	0.84	4.96	1.07	2.96	0.46	2.75	0.43	3.09	0.27	1.79	0.53	0.20
D156.4	2.7	376	27	139	5.0	0.18	60	7.92	20.17	3.03	14.63	3.93	1.41	4.36	0.75	4.48	0.94	2.62	0.39	2.42	0.39	3.03	0.36	2.06	0.50	0.43
DF32	3.9	196	53	230	5.7	0.30	45	8.37	26.02	4.35	20.35	6.21	1.91	7.25	1.29	8.22	1.78	5.13	0.81	4.90	0.72	5.41	0.40	2.22	0.50	0.39
PD7	3.8	244	48	256	5.5	0.22	61	10.3	28.65	4.52	22.11	5.99	1.93	6.95	1.27	7.67	1.67	4.76	0.74	4.57	0.71	5.68	0.39	2.52	0.73	0.40

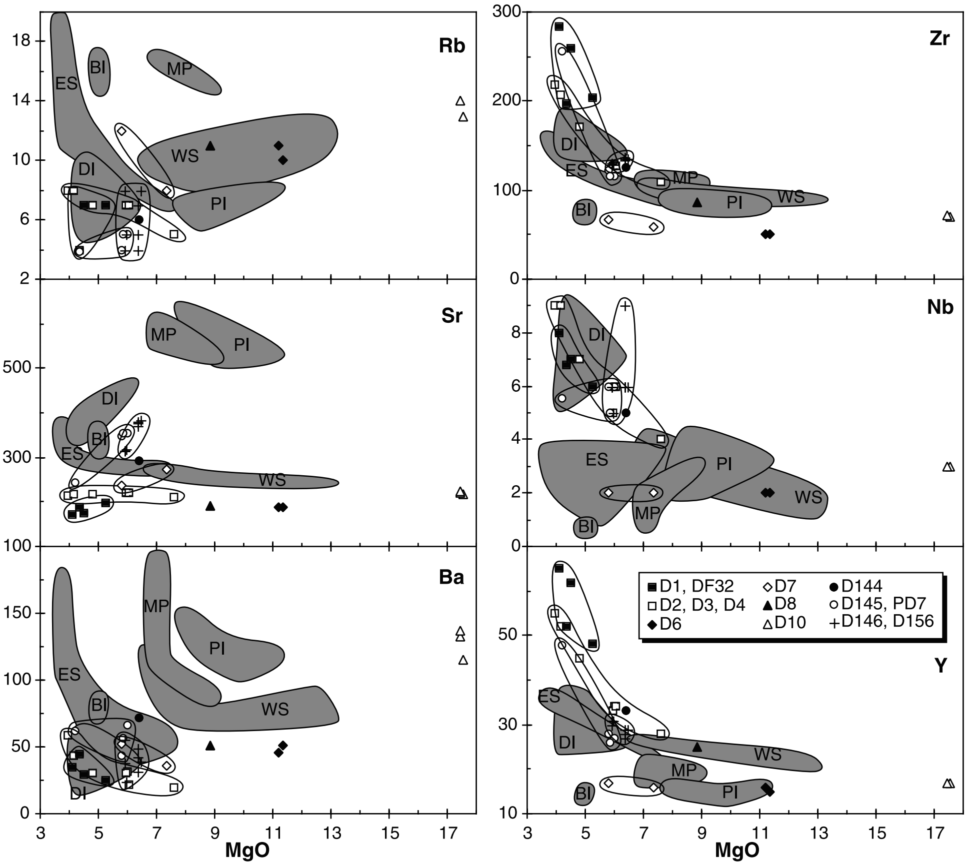

Figure 5. Whole rock MgO versus trace elements plots for Bransfield Strait volcanism. Shaded fields are published data [from *Keller and Fisk*, 1992; *Keller et al.*, 1992] for other Bransfield Strait locations (abbreviations as in Figures 3 and 4). Values are in wt % for MgO and ppm for trace elements.

geochemical deviations from MORB are typical of lavas that have been influenced by a subduction zone [*Pearce and Parkinson*, 1993].

[24] Samples from the westernmost dredged feature (D145, D146, and D156, and piston core PD7) have noticable Cs, Ba, U, K, Pb, and Sr spikes (although the Sr spike on PD7 was presumably removed by plagioclase fractionation) and Nb-Ta depletions (Figure 6e), although none of these characteristics are as pronounced as they are in the arc or in samples from D6 and D7 (see below). Stepping eastward, samples from D1 and piston core DF86.32 (both from the same volcanic feature at 59°W) have spikes at Cs, K, and Pb, and possibly U but lack the Ba, Th, and Sr enrichments of the arc samples (Figure 6b). Their Nb-Ta depletion is noticable, but not nearly as pronounced as that of the arc. D144.4, also from the same feature, has a Nb-Ta depletion similar to that of D1 but has more pronounced K and Pb spikes and Ba and Sr spikes that D1 lacks. However, the higher Sr of D144.4 may be partially due to the fact that it is less evolved than any of the D1 samples and experienced less plagioclase fractionation.

[25] Stepping farther eastward, samples from D2–D4 (all from the same feature at 58.4°W) have Cs, Ba, K, Pb, and Sr enrichments and Nb-Ta depletions similar to D1 (Figure 6c), although Sr enrichments seen in the least evolved samples in D2–D4 do not continue into the more evolved samples due to plagioclase fractionation. Moving eastward again, samples from D6–D8 and D10 have more of the arc characteristics than any of the other dredges (Figure 6d). D6 and D7 have the lowest REE concentrations of any dredged sample and have among the highest concentrations of the arc characteristic elements: their Cs, K, Pb, and Sr enrichments and Nb-Ta depletions are unmatched by the other dredged samples and, in fact, exceed some of the arc samples in relative magnitude. D6 and D7 are also enriched in Ba, but this is partially disguised by an enrichment in Rb that is unique among the dredged samples (except for D8, see below). The P depletion seen in D6 and D7 is much less prominent in the other dredged samples, but P depletion is also not a consistent characteristic of the six arc samples analyzed. D8 has enrichments in Cs, Rb, Ba, K, Pb, and Sr, but its depletion in Nb-Ta (Figure 6d) is more subdued than in D6 and D7, although more pronounced than the other dredged samples. D10, despite having relatively high MgO (6.5 wt % in glass, 17.6 wt % in whole rock) and low heavy rare earth element (REE) concentrations, has the highest Ba, Th, and U, and among the highest Pb and K, and a steep REE pattern (Figure 6d). With the exception of its high Rb it is quite similar to some of the arc samples.

[26] It is difficult to compare the new samples to the subaerial volcanism in Bransfield Strait because compre-

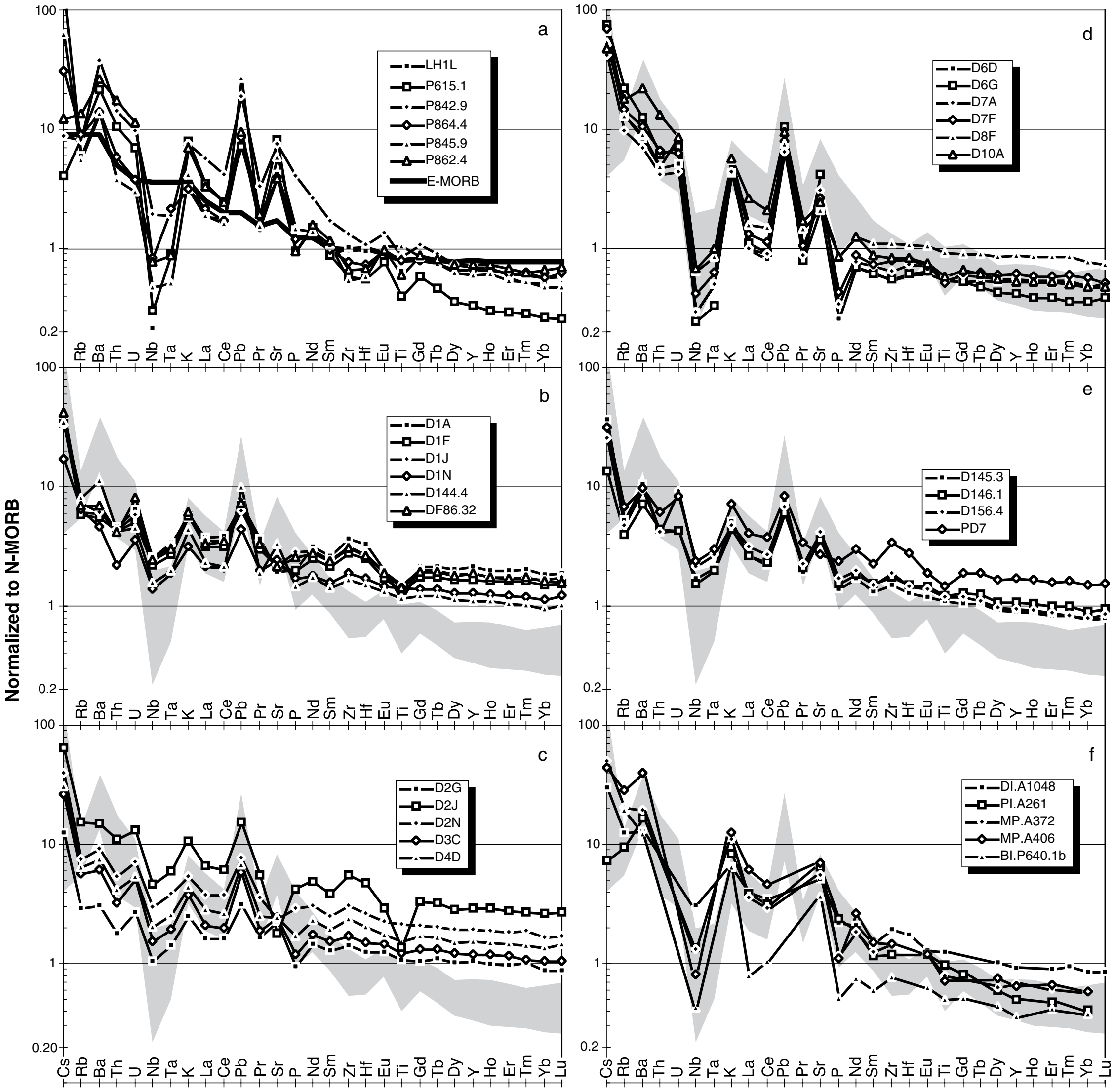

Figure 6. NMORB-normalized multielement plots of (a) South Shetland Island arc and (b–f) Bransfield Strait samples (normalized to NMORB values of *Sun and McDonough* [1989]). The thick line in Figure 6a is the EMORB of *Sun and McDonough* [1989]. The shaded field in Figures 6b–6f is the South Shetland Arc data from Figure 6a for comparison. Abbreviations are as in Figures 3 and 4. Data sources are as in Figure 4, except some Bridgeman Island data from *Weaver et al.* [1979]. Sample LH1L is a 24 Ma basalt from King George Island [*Keller et al.*, 1992]. Normalizing values are from *Sun and McDonough* [1989].

hensive trace element data for the subaerial volcanoes are rare [*Weaver et al.*, 1979; *Keller et al.*, 1992]. There are no published Pb concentration data, for example, so it is not known if the subaerial volcanoes have the characteristic Pb enrichment of the arc. From what data are available it is apparent that the subaerial volcanoes have a complex combination of arc and non-arc characteristics (Figure 6f). Deception Island has noticable Cs and Sr spikes, but a subdued K spike, no Ba spike, and little or no Nb depletion. Penguin Island has spikes at Ba, K, and Sr and a depletion at Nb, all of which are arc characteristics, but its relative depletion at Cs is opposite to what is found in the arc. Penguin Island also has the steepest REE pattern of any Bransfield Strait volcano [*Weaver et al.*, 1979]. Melville Peak has nearly all of the chemical characteristics of the arc, such as the highest Cs, Ba, K, and Sr, and among the lowest Nb of any subaerial Bransfield Strait volcano, but its Rb, K, and LREE contents are higher than the arc. Bridgeman Island has higher Rb and lower P_2O_5, LREE, and MREE contents than the arc, but otherwise has incompatible trace element characteristics similar to the arc.

4.3. Isotopes

[27] The only previously published Sr-Nd-Pb isotopic data from the South Shetland Arc are for a 24 Ma basalt from King George Island [*Keller et al.*, 1992]. For this study, we analyzed additional samples from King George, Robert, and Livingston Islands (Figure 2 and Table 4). The

Table 4. Isotopic Data for Basalts From the South Shetland Island Arc[a]

	Sample				
	P615.1	P842.9	P864.4	P845.9	P862.4
	Measured Ratios				
$^{87}Sr/^{86}Sr$	0.70319 (0.7032)	0.70397	0.70428 (0.7042)	(0.7039)	(0.704)
$^{143}Nd/^{144}Nd$	0.51303 (0.513)	0.51281	(0.5128)	(0.5129)	(0.5128)
$^{206}Pb/^{204}Pb$	18.532	18.616	18.617	18.585	18.891
$^{207}Pb/^{204}Pb$	15.567	15.581	15.581	15.587	15.619
$^{208}Pb/^{204}Pb$	38.196	38.312	38.353	38.313	38.726
K-Ar age, Ma	51	82	95	109	123
	Age-Corrected (Initial) Ratios				
$^{87}Sr/^{86}Sr$	0.70317	0.70394	0.70423	0.7039	0.7039
$^{143}Nd/^{144}Nd$	0.51299	0.51274	0.51272	0.51274	0.51267
$^{206}Pb/^{204}Pb$	18.446	18.543	18.544	18.564	18.636
$^{207}Pb/^{204}Pb$	15.563	15.578	15.577	15.586	15.607
$^{208}Pb/^{204}Pb$	38.092	38.224	38.262	38.291	38.404

[a] Locations are given in Table 2. Isotopic ratios were measured at Cornell University (except those in parentheses were measured at NERC-BAS) using procedures described by *White et al.* [1990]. See Appendix A for analytical details and standard errors. K-Ar dates [*Smellie et al.*, 1984] and ICP-MS trace element data (Table 3) were used for age corrections.

samples represent a range of ages and locations on the South Shetland Islands and provide a useful comparison with the volcanism in Bransfield Strait (Table 5). The youngest arc sample (24 Ma) is isotopically indistinguishable from some of the Bransfield Strait samples, but the other arc samples have lower $^{206}Pb/^{204}Pb$ and $^{207}Pb/^{204}Pb$, and all but the 24 Ma and 51 Ma samples have lower $^{143}Nd/^{144}Nd$ and higher $^{87}Sr/^{86}Sr$ (Figure 7) than do the Bransfield Strait samples.

[28] Of the Bransfield Strait samples, dredges D1–D4 have the lowest $^{87}Sr/^{86}Sr$ and among the highest $^{143}Nd/^{144}Nd$ and are thus the most similar to the depleted upper mantle values found at mid-ocean ridges. These same samples have among the highest $^{206}Pb/^{204}Pb$ values found in Bransfield Strait, although they are still within the reported range of MORB. Dredges D144–D156 are mostly similar to D1–D4, although not quite as depleted. Samples from the northeast end of the rift (e.g., D6–D8, D10) tend to have more enriched Sr and Nd isotopic ratios, i.e., displaced toward the arc values. D10, for example, has the highest $^{87}Sr/^{86}Sr$ and lowest $^{143}Nd/^{144}Nd$ of any dredged sample. The subaerial Bransfield Strait samples tend to have more of a subduction signature than the dredged samples: Penguin Island has the highest $^{87}Sr/^{86}Sr$, Melville Peak has the lowest $^{206}Pb/^{204}Pb$,

Table 5. Isotopic Data for Samples Dredged From Bransfield Strait[a]

Sample	$^{87}Sr/^{86}Sr$	$^{143}Nd/^{144}Nd$	$^{206}Pb/^{204}Pb$	$^{207}Pb/^{204}Pb$	$^{208}Pb/^{204}Pb$
D1A	0.70276	0.51308	–	–	–
D1F	0.70277	0.51306	18.771	15.592	38.426
D2G	0.70274	0.51307	18.763	15.564	38.332
D2N	0.70288	0.51304	18.744	15.577	38.382
D3C	0.70304	0.51304	18.766	15.600	38.480
D4D	0.70300	0.51306	18.769	15.602	38.473
D6D	0.70345	0.51294	18.746	15.595	38.520
D7A	0.70336	0.51301	18.724	15.585	38.455
D8F	0.70326	0.51302	18.744	15.587	38.473
D10A	0.70370	0.51293	18.748	15.602	38.533
D144.1	0.70290	0.51305	18.740	15.571	38.356
D144.4	0.70337	0.51306	18.723	15.582	38.431
D145.3	0.70329	0.51303	18.696	15.584	38.387
D156.4	0.70313	0.51305	18.710	15.577	38.353

[a] See Appendix A for analytical details and standard errors.

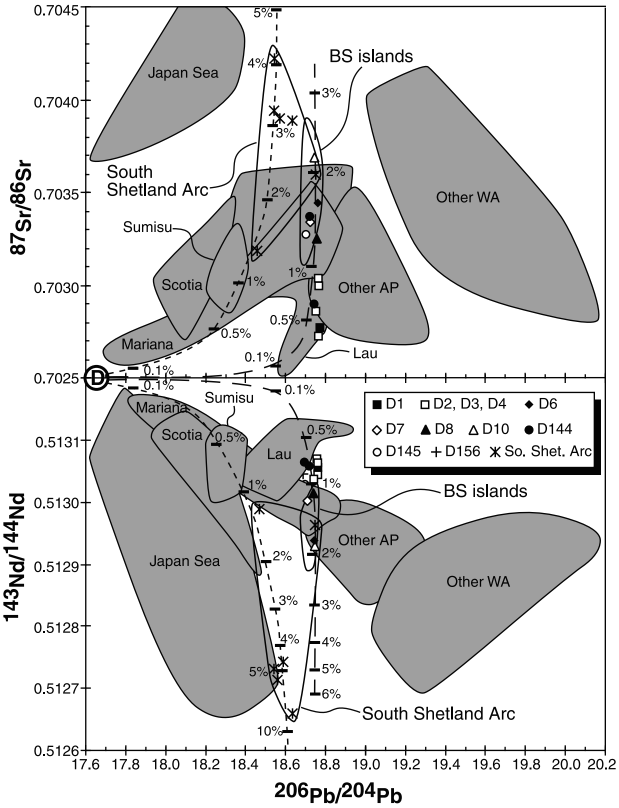

Figure 7. The ratios $^{206}Pb/^{204}Pb$ versus $^{87}Sr/^{86}Sr$ and $^{143}Nd/^{144}Nd$ of South Shetland Island Arc and Bransfield Strait samples (data from Tables 4 and 5 and *Keller et al.* [1992]) compared to published data from other back arc basins (see text for data sources). The long-dashed line is a calculated mixing line between a depleted mantle component (shown by large D) with Sr ppm = 20, $^{87}Sr/^{86}Sr$ = 0.7025, Nd ppm = 1.1, $^{143}Nd/^{144}Nd$ = 0.5132, Pb ppm = 0.043, and $^{206}Pb/^{204}Pb$ = 17.6 and a subducted metalliferous sediment component with very high Pb concentration (Pb ppm = 200, $^{206}Pb/^{204}Pb$ = 18.75), high $^{87}Sr/^{86}Sr$ (= 0.709), low $^{143}Nd/^{144}Nd$ (= 0.5124), and very low Sr/Pb (≤ 1, Sr ppm = 200) and Nd/Pb (= 0.1, Nd ppm = 20). The short-dashed line represents mixing between D and South Atlantic sediment [from *Ben Othman et al.*, 1989]. Tick marks on the mixing lines are labeled with the percentage of the sediment component. A mixing line between depleted mantle with a higher $^{206}Pb/^{204}Pb$ of 18.75 and South Atlantic sediment would be a vertical line and would match the long-dashed mixing line at sediment percentages >0.5%. Fields shown are (see text for references) Japan Sea, Sumisu Rift, East Scotia Sea, Lau Basin, Mariana Trough, Bransfield Strait islands (BS islands [*Keller et al.*, 1992]), other locations on the Antarctic Peninsula (AP [*Hole*, 1990; *Hole et al.*, 1993]), and other locations in West Antarctica (WA [*Hart et al.*, 1995; *Rocholl et al.*, 1995]). Published data for the Bransfield Strait seamounts (ES and WS of previous figures [*Keller et al.*, 1992]) fall in the middle of the field described by these new data but have been omitted for clarity.

and Bridgeman Island has the lowest $^{143}Nd/^{144}Nd$. Deception Island falls in the middle of the range of the rest of the samples, except for its high $^{207}Pb/^{204}Pb$ and $^{208}Pb/^{204}Pb$.

5. Discussion

5.1. Variations in the "Arc Component"

[29] The tectonic setting of a back arc basin above mantle that has been variably affected by dehydration/melting at a subduction zone can give back arc basalts compositions that lie between a depleted upper mantle signature and a subduction zone signature. The chemical signature of depleted upper mantle is easier to identify because of its relatively consistent geochemical characteristics, but the subduction zone signature varies from arc-to-arc, making the subducted component harder to identify and interpret. Our analyses of the six South Shetland arc basalts provide a general sense of the chemical characteristics of the subduction zone volcanism in this area.

[30] As noted earlier, the South Shetland arc samples have high Ba and Pb and low Nb and Ta (Figure 6a). These chemical characteristics are common features of arc volcanism in general [e.g., *Pearce and Parkinson*, 1993] and make high Ba/Nb and low Ce/Pb good indicators for an arc component in BAB volcanism. The Bransfield Strait dredges and South Shetland Arc samples fall along a mixing curve in Ba/Nb-Ce/Pb space, with the arc samples at high Ba/Nb-low Ce/Pb and the most depleted Bransfield Strait samples at low Ba/Nb-high Ce/Pb (Figure 8a). Samples dredged from the northeast end of the Bransfield rift (D6–D8, D10) have Ba/Nb values that overlap the low end of the arc field and Ce/Pb values the same as the arc. Samples dredged from elsewhere along the rift have lower Ba/Nb and higher Ce/Pb and thus have less of the arc component than D6–D10. The two dredges with the smallest arc signature (D1 and D2) have low Ba/Nb and the highest Ce/Pb and the lowest $^{87}Sr/^{86}Sr$ and highest $^{143}Nd/^{144}Nd$. Their maximum Ce/Pb (14) is less than the Ce/Pb of typical MORB (~25 [*Sun and McDonough*, 1989]) because the Bransfield Strait samples have higher Pb contents (1–3 ppm versus <1 ppm for MORB). Substituting U/Nb for Ba/Nb in Figure 8a produces a virtually identical plot.

[31] The enrichment of the South Shetland arc samples in Sr and Ba is obvious even in comparison to alkaline elements. For example, at any given K/Rb the arc has higher Ba/Rb (Figure 8b) and Sr/Rb than do the dredged samples, suggesting that the sub-arc mantle has been preferentially enriched in Sr and Ba by the subducted slab.

[32] Two unusual isotopic characteristics of the Bransfield Strait basalts provide clues to the nature of the mantle source beneath Bransfield Strait and the importance of the subducted component there: the apparent lack of a low-$^{206}Pb/^{204}Pb$ depleted component that exists in other BABs and the narrow range of Pb isotopic ratios compared to Sr and Nd isotopic ratios (Figure 7). There are at least two possible explanations for these unusual isotopic characteristics:

1. Unlike in other BABs, the depleted mantle beneath Bransfield Strait has Pb isotopic ratios that are at the high end of the MORB range and similar to the Pb isotopic ratios of the arc component. Other basaltic volcanism in this part of West Antarctica tends to have even higher $^{206}Pb/^{204}Pb$

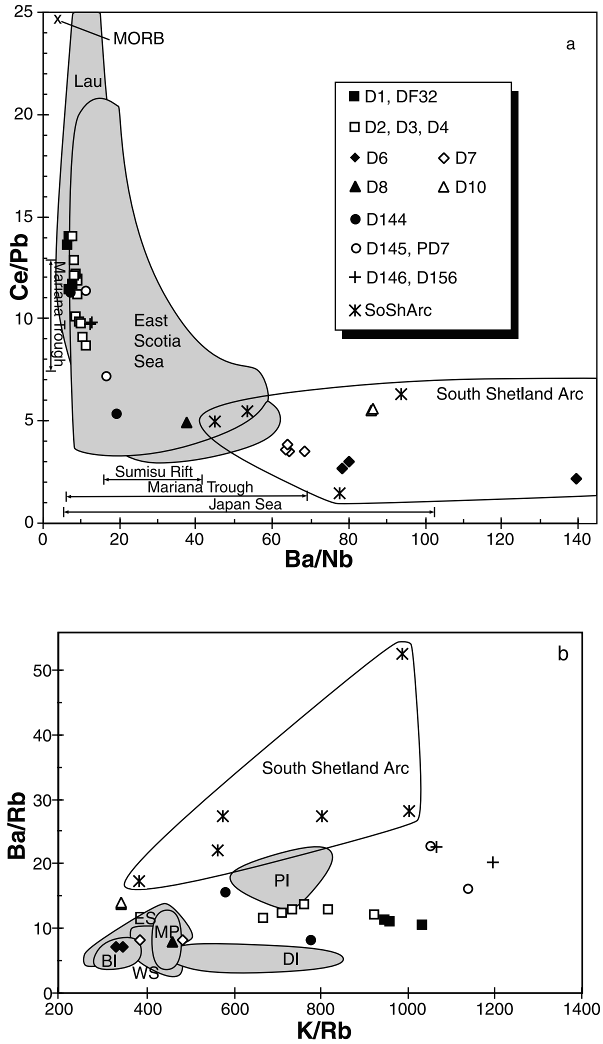

Figure 8. (a) Ba/Nb versus Ce/Pb and (b) K/Rb versus Ba/Rb of South Shetland Island Arc and Bransfield Strait samples. Abbreviations are as in Figure 2. Data from other back arc basins (see text for references) are shown for comparison. MORB value in Figure 8a is from *Sun and McDonough* [1989].

[*Hole et al.*, 1993; *Hart et al.*, 1995], although the isotopic data plot close to a straight line, which argues against single-stage, three-component mixing, but is consistent with multistage mixing where the high-$^{206}Pb/^{204}Pb$ component was mixed in before the high-$^{87}Sr/^{86}Sr$ component.

2. Low-$^{206}Pb/^{204}Pb$ mantle similar to that found at other BABs (including the nearby East Scotia Sea) may exist beneath Bransfield Strait, but the Bransfield Strait volcanism only samples sources that have been thoroughly contaminated by subducted Pb. Pb concentrations would have to be so much higher in the subducted sediments than in the mantle that incorporation of <1% bulk sediment gives the mantle-sediment mixture the Pb isotopic composition of the sediments while barely affecting the Sr and Nd isotopic compositions. Incorporation of additional sediment beyond the first 1% has little further affect on the Pb isotopic ratios, and only changes the Sr and Nd isotopic ratios, resulting in a vertical array of data in Pb-Sr or Pb-Nd isotopic space.

The dashed line in Figure 7 is a mixing curve that illustrates this point. *Keller et al.* [1992] favored this model for the dredged and subaerial Bransfield Strait samples they analyzed. However, their explanation is strained by the more recently dredged basalts, some of which have even lower $^{87}Sr/^{86}Sr$ (0.7027), but Pb isotopic compositions similar to the other Bransfield Strait samples. These low-$^{87}Sr/^{86}Sr$ samples fall off of the mixing line in Figure 7 but can be modeled with a mixture of low-$^{206}Pb/^{204}Pb$ mantle and sediments with higher Pb concentrations ($\geq$200 ppm) and lower Sr/Pb ($\leq$1) than any known sediment except for Mn nodules [*Ben Othman et al.*, 1989]. We note, however, that what we are calling here a sediment component is more likely a sediment-derived fluid [e.g., *Stolper and Newman*, 1994] that could have an even higher Pb concentration.

[33] Regardless of which of these two models we prefer, the subduction component must have high $^{87}Sr/^{86}Sr$ and low $^{143}Nd/^{144}Nd$, and Pb isotopic ratios similar to those of the Bransfield Strait samples. This explains why all of the Bransfield Strait samples have similar Pb isotopic ratios and also why the samples with the strongest arc signatures in their trace elements (D6, D7, D8, D10) also have the most arc-like Sr and Nd isotopic ratios.

5.2. Along-Axis Variations

[34] BABs that have along-axis variations in rift morphology can also have along-axis variation in basalt chemistry, such that the more mature (wider) parts of the rift tend to erupt basalts more similar to MORB [*Saunders et al.*, 1982; *Hawkins*, 1995]. However, in Bransfield Strait, two additional factors must be kept in mind: Any along-axis variation may be complicated by the two anomalously large on-axis volcanoes of Deception and Bridgeman Islands. Moreover, our submarine samples from the southwest section of the rift are from large edifices, while our submarine samples from the northeast half of the rift are mostly from small features. Looking just at the submarine samples, there are variations in incompatible elements that suggest a greater contribution from a depleted, more MORB-like, source at the southwest end of the rift. The axial ridge at 59.0°W (samples D1, D144, and DF32), which resembles a relatively mature rift feature, has the most MORB-like (depleted) trace element concentrations and Sr-Nd isotopic ratios of any sampled feature. In general, dredges from the southwest end of the rift tend to have lower K_2O/P_2O_5 and higher K/Rb and Ba/Rb than the other dredges (Figure 9) (but Ba/Rb lower than the arc; Figure 8b). Neglecting Deception Island, K_2O contents actually decrease toward the southwest end of the rift, but Rb concentrations decrease even more, which raises K/Rb ratios of the southwest dredges (0.10–0.14) to typical values for NMORB (0.13 [*Sun and McDonough*, 1989]). This suggests that depleted mantle similar to a MORB source is more important at the southwest end of the rift.

[35] P_2O_5 also increases to the southwest despite decreasing K_2O, and the low K_2O/P_2O_5 values in the southwest are also similar to NMORB (0.62 [*Sun and McDonough*, 1989]). Additional MORB-like features of the southwest dredged samples are their high Na_2O/K_2O and $^{143}Nd/^{144}Nd$ and low Rb/Sr and $^{87}Sr/^{86}Sr$. Although some of the low trace element ratios could be due to in situ depletion of the Bransfield Strait source by repeated melting during rifting, the depleted isotopic ratios relative to those farther northeast require that a long-term-depleted reservoir, such as oceanic upper mantle, is making a larger contribution to the southwestern Bransfield Strait source.

[36] Nb concentrations are higher in the southwest, including Deception Island (Nb as high as 9 ppm at MgO contents similar to the dredged samples). This increase in Nb could be associated with the increasing contribution from MORB-like mantle in the southwest, or it could be due to a change in melting conditions. H_2O is known to increase the distribution coefficient of Nb in mafic systems [*Tatsumi et al.*, 1986], so higher H_2O in the source in the northeast would cause Nb to be less incompatible there and thus in lower concentrations in the melts. Evidence for a more hydrous source region in the northeast includes the higher degree of melting at

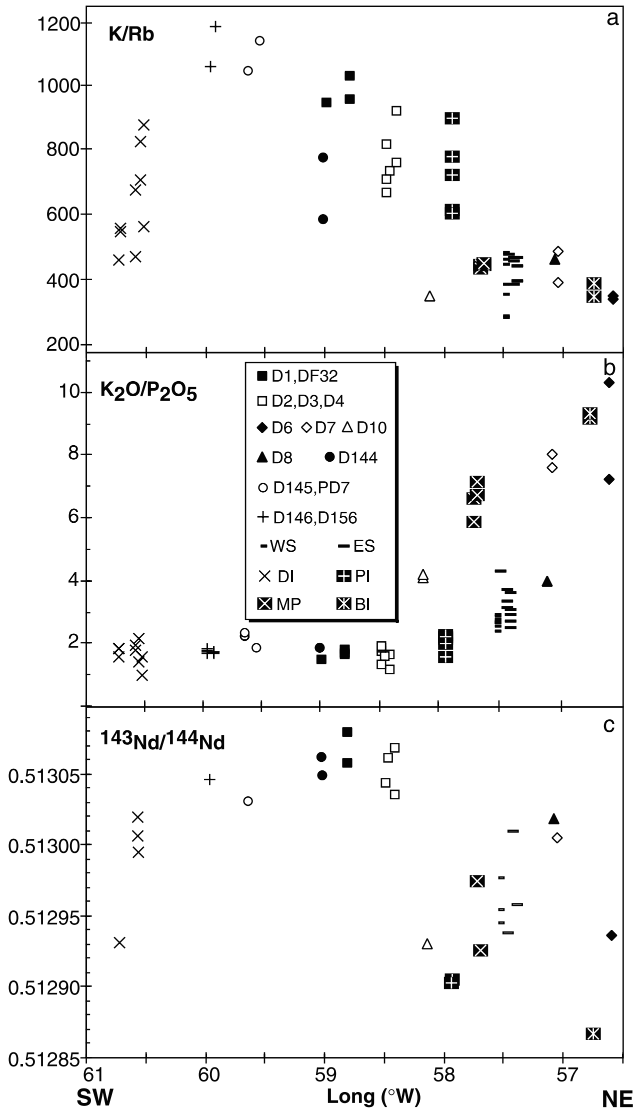

Figure 9. Longitude versus (a) K/Rb, (b) K_2O/P_2O_5, and (c) $^{143}Nd/^{144}Nd$ for Bransfield Strait samples. Abbreviations are as in Figure 4. Data sources are as in Figure 4 except Rb data for dredges are ICP-MS data only.

Bridgeman Island and the northeast dredged samples (suggested by their lower Ce/Y [*Weaver et al.*, 1979; *Keller et al.*, 1992]) and the fact that samples dredged in the northeast tend to be more vesicular.

5.3. Comparisons to Other Back Arcs

[37] Much of what we know about the formation of BABs has come out of geophysical and geological surveys of BABs in the western Pacific, e.g., the Japan Sea, Lau Basin, Mariana Trough, and Sumisu Rift. Comparing Bransfield Strait to these other BABs may help us understand how Bransfield Strait's continental tectonic setting and rift-to-drift transitional nature affect the volcanism there.

[38] The Japan Sea is similar to the Bransfield Strait in that it is also ensialic, but the Japan Sea differs in that it is wider, better developed, and no longer active [*Tamaki et al.*, 1992]. Some trace element characteristics of the Japan Sea are similar to those of Bransfield Strait (e.g., Ba/Nb 6–103 for Japan Sea versus 6–140 for Bransfield Strait; Figure 8a), but the two areas have significantly different isotopic characteristics. Pb isotopic ratios of Japan Sea basalts extend from values similar to those for the Bransfield Strait down to values much lower than anything in Bransfield Strait (Figure 7). Sr isotopic ratios of Japan Sea basalts, including those with low Pb isotopic ratios, are higher than those of Bransfield Strait basalts. Japan Sea Nd isotopic ratios extend to both higher and lower values. The high-$^{87}Sr/^{86}Sr$ end-member in Japan Sea basalts has been identified as subducted sediments [*Cousens and Allan*, 1992; *Cousens et al.*, 1994; *Pouclet et al.*, 1995], but these sediments must be very different isotopically from the sediments contributing to the high-$^{87}Sr/^{86}Sr$ Bransfield Strait end-member. The higher Sr isotopic ratios of Japan Sea basalts require that the subducted component at the Japan Sea has higher Sr concentrations and/or $^{87}Sr/^{86}Sr$ and/or is present in greater percentages in the Japan Sea source than in the Bransfield Strait source.

[39] BABs in the western Pacific are at various stages of development: from a very young back arc rift lacking an axial neovolcanic ridge (Sumisu Rift at 31°N [*Taylor et al.*, 1990]) to a more mature BAB that has been spreading for at least 3 Myr and has an axial neovolcanic ridge with segments up to 65 km long (Mariana Trough at 18°N [*Hawkins et al.*, 1990]) to an even more mature BAB that has been spreading for 5 Myr (Lau Basin at 20°S [*Hawkins*, 1995]). The width of Bransfield Strait and the presence of <30-km-long axial ridges there appear to place it somewhere between Sumisu Rift and MT in this spectrum of tectonic development. The relative tectonic development of Bransfield Strait compared to oceanic BABs of the western Pacific is mirrored by the composition of Bransfield Strait volcanism compared to those other BABs.

[40] Sumisu Rift basalts fall in the middle of the Bransfield Strait range of trace element characteristics and are neither as arc-like nor as MORB-like. For example, Sumisu Rift Ba/Nb ranges from 16 to 42 (Figure 8a) [*Hochstaedter et al.*, 1990], compared to the Bransfield Strait range of 6–140. No published Pb concentration data are available for Sumisu Rift, but Pb isotopic ratios are all markedly lower in the Sumisu Rift [*Hochstaedter et al.*, 1990] than in Bransfield Strait (Figure 7). The two areas have similar $^{143}Nd/^{144}Nd$, but Sumisu Rift has a narrower range of $^{87}Sr/^{86}Sr$ at mid-Bransfield Strait values.

[41] Trace element ratios in Mariana Trough basalts [*Hawkins et al.*, 1990; *Stern et al.*, 1990] are similar to the most MORB-like (southwestern) Bransfield Strait dredges (Figure 8a): the maximum Ce/Pb in Mariana Trough (13) is similar to the Bransfield Strait maximum (14), but Mariana Trough Ba/Nb does not exceed 70, while northeastern Bransfield Strait samples have Ba/Nb as high as 140. Isotopic ratios of the enriched ends of the Mariana Trough isotopic fields [*Hawkins et al.*, 1990; *Stern et al.*, 1990; *Volpe et al.*, 1990] are similar to Bransfield Strait isotopic ratios (Figure 7), but the depleted end of Mariana Trough isotopic fields extend to lower Sr and Pb isotopic ratios and higher Nd isotopic ratios than Bransfield Strait.

[42] Some of the basalts in the Lau Basin are more MORB-like than anything found in Bransfield Strait and are virtually indistinguishable from NMORB [*Hawkins*, 1995]. Ba/Nb does not exceed 60 in Lau Basin [*Hergt and Farley*, 1994; *Pearce et al.*, 1995], which is lower than the northeastern Bransfield Strait dredged samples (Figure 8a). Lau Basin Ce/Pb values range from similar to MORB (>20) to similar to the northeastern Bransfield Strait dredged samples (<5). The most enriched Sr, Nd, and Pb isotopic ratios of Lau Basin basalts [*Volpe et al.*, 1988; *Hergt and Farley*, 1994; *Hergt and Hawkesworth*, 1994] overlap the Bransfield Strait field (Figure 7), but once again, the Lau Basin fields extend to ratios more MORB-like than anything in Bransfield Strait.

[43] The BAB in the East Scotia Sea is geographically the closest to Bransfield Strait, but it has been spreading for 8 Myr [*Barker and Hill*, 1981] and is much wider and more mature than Bransfield Strait. The East Scotia Sea has more MORB-like trace element ratios (Ce/Pb up to 20, and Ba/Nb <70 [*Saunders and Tarney*, 1979; *Cohen and O'Nions*, 1982; *Leat et al.*, 2000]) than Bransfield Strait (Figure 8a). Sr and Nd isotopic ratios in East Scotia Sea are similar to the Bransfield Strait seamount values, although the East Scotia Sea data extend to slightly higher $^{143}Nd/^{144}Nd$, and the Bransfield Strait data extend to slightly higher $^{87}Sr/^{86}Sr$ (Figure 7). Pb isotopic ratios in East Scotia Sea are markedly lower than and do not overlap Bransfield Strait ratios. The East Scotia Sea spreading center is clearly sampling a depleted end-member that is not evident in the Bransfield Strait samples. Moreover, that depleted end-member in the East Scotia Sea is different from the depleted end-member of the western Pacific BABs, especially in its lower $^{208}Pb/^{204}Pb$.

[44] Only the Mariana Trough and Lau Basin include basalts with $^{87}Sr/^{86}Sr$ lower than anything found in Bransfield Strait, but all the other BABs include basalts with Pb isotopic ratios lower than anything in Bransfield Strait. The Japan Sea data show that we cannot attribute the higher Pb isotopic ratios in Bransfield Strait uniquely to its ensialic setting. It is possible that the depleted mantle end-member beneath Bransfield Strait has inherently higher Pb isotopic ratios (although still within the MORB range) than the depleted mantle beneath the other BABs. However, we cannot rule out the possibility that there is a depleted end-member beneath Bransfield Strait with low Pb isotopic ratios but that the subducted component has such high Pb

concentrations and low Sr/Pb values that it can dominate the Pb isotopic signature of Bransfield Strait volcanism without having much affect on the Sr and Nd isotopes.

6. Conclusions

[45] Bransfield Strait is unique among back arc basins in that it is both actively forming within continental crust and in the transition from rifting to spreading. Trace element characteristics of newly dredged samples range from very similar to the nearby arc volcanism to very similar to mid-ocean ridge basalts. In the most MORB-like Bransfield Strait basalts, only high Cs and Pb (and to a lesser extent K and Ba) concentrations and slightly low Nb and Ta concentrations are noticeably different from MORB. Sr, Nd, and Pb isotopic ratios extend from enriched values similar to the arc, to depleted values within the range of MORB, although Pb isotopic ratios are at the high end of the MORB range. Large-ion lithophile element (LILE) and isotopic depletion of the Bransfield Strait basalts relative to NMORB is an approximate function of the developmental maturity of the features from which they were collected. However, the volcanic and geochemical variations are not systematic along-axis and thus do not reflect the unidirectional propagation of rifting suggested by geophysical data [*Barker and Austin*, 1998].

[46] Bransfield Strait has a narrow range of Pb isotopic ratios for its range of Sr and Nd isotopic ratios, and there is no evidence of the low-$^{206}Pb/^{204}Pb$ component found in all other back arc basins. Mixing calculations require either that the depleted mantle isotopic component beneath Bransfield Strait has relatively high $^{206}Pb/^{204}Pb$ (similar to $^{206}Pb/^{204}Pb$ in the South Shetland arc) or that the depleted component has low $^{206}Pb/^{204}Pb$ and the subducted component has such high Pb concentration and low Sr/Pb ($\leq$1) that it dominates the Pb isotopic signature of the BAB even at very small amounts of mixing.

Appendix A: Analytical Techniques

[47] The glass analyses presented here were determined by electron microprobe at Oregon State University using a four-spectrometer Cameca SX-50. Makaopuhi basalt glass from the Smithsonian reference collection was the standard. Software provided with the microprobe corrected for atomic number, absorption, and fluorescence effects. Glass was analyzed with 15-kV accelerating voltage, 30-nA beam current, and 10-s counting times, except Ti and Al were counted for 20 s. Na was always analyzed first and showed no evidence for loss under these conditions. Precision based upon multiple analyses of the Makaopuhi basalt glass is reported by *Forsythe and Fisk* [1994].

[48] The whole rock major and trace element data presented in Table 2 were determined by X-ray fluorescence (XRF) at NERC-BAS, Cambridge, UK, using techniques described by *Smellie et al.* [1995].

[49] Trace element and rare earth element data were analyzed by inductively coupled plasma mass spectrometry (ICP-MS) at Oregon State University. Approximately 70 mg of <1 mm, clean chips were hand-picked, rinsed in deionized water, and dried in an 80 °C oven. The chips were then digested overnight in a mixture of redistilled GFS HF and doubly distilled 8 N HNO_3 in sealed Savilex™ capsules in a 80°C oven. The capsules were then opened and the solutions allowed to dry on a 70°C hotplate in an exhaust hood. When dry, 0.5 mL of 6 N HCl was added and allowed to dry down. Then 0.5 mL of 8 N HNO_3 was added and allowed to dry down, and this step was then repeated. The residue was then taken up in 10 mL of 2 N HNO_3. This solution was then diluted 20:1 with 1% HNO_3 and placed in a run tube with a Be-In-Re-Bi spike.

[50] Before running rock solutions on the VG PlasmaQuad PQ2 + ICP-MS, a sample rock solution is used to tune the machine for maximum response to the elements sought. The unknown solutions are then run in suspected order of increasing trace element concentrations. The analysis procedure used is a 75-s uptake, 60-s acquire, and 150-s wash. Three consecutive replicates are done on each sample solution. The PlasmaQuad calculates and prints out integrated counts per second (cps) for each element. The cps from each of these three replicates are then checked for flyers and averaged.

[51] Instrument drift is monitored and corrected using the Be-In-Re-Bi spike and a monitor solution that is analyzed 8–10 times during the course of an 8-hour run. Matrix affects are minimized by using consistent sample weights but are also monitored via the Be-In-Re-Bi spike. Corrected counts are then converted to concentrations using a linear regression of at least four international rock standards (e.g., AGV-1, BCR-1, BHVO-1, JB-1, and W-2).

[52] Isotopic ratios of Sr, Nd, and Pb were measured at Cornell University using procedures described by *White et al.* [1990]. All samples were leached repeatedly in hot HCl prior to digestion, and all isotopic ratios were corrected for fractionation. Sr and Pb isotopic ratios were referenced to standards NBS987 (=0.710248) and NBS981 (=16.937, 15.493, 36.705), respectively. The average $^{143}Nd/^{144}Nd$ for the La Jolla Nd standard measured at the time of these analyses was 0.511856 ± 15. Two-sigma standard errors based upon numerous analyses of standards during the time of the unknown runs are $^{87}Sr/^{86}Sr \pm 0.000012$, $^{143}Nd/^{144}Nd \pm 0.000015$, $^{206}Pb/^{204}Pb \pm 0.005$, $^{207}Pb/^{204}Pb \pm 0.007$, and $^{208}Pb/^{204}Pb \pm 0.017$. Within-run standard errors due to machine precision are smaller than these between-run errors.

[53] **Acknowledgments.** Dredging in Bransfield Strait was supported by NSF grants DPP90-19247 to L. Lawver and OPP93-17361 to G. Klinkhammer. We are grateful to P. Barker and C. Chin for helping to obtain additional dredge samples in Bransfield Strait. J. Anderson provided sample DF86.32. Analytical work was supported by NSF grants DPP88-17126 and OPP93-17307 to M. Fisk. We are grateful to I. Millar for providing some of the Sr-Nd isotopic data in Table 4, to R. Nielsen for assisting with the microprobe analyses, and to A. Ungerer for assisting with the ICP-MS analyses. J. Allan, J. Pearce, and R. Stern provided helpful reviews of the manuscript.

References

Anderson, J. B., D. J. DeMaster, and C. A. Nittrover, Preliminary results from marine geological cruises aboard the U. S., *Coast Guard icebreaker Glacier, Antarct. J. U. S.*, *22*, 144–148, 1987.

Barker, D. H. N., and J. A. Austin Jr., Crustal diapirism in Bransfield Strait, West Antarctica—Evidence for distributed extension in marginal basin formation, *Geology*, *22*, 657–660, 1994.

Barker, D. H. N., and J. A. Austin Jr., Rift propagation, detachment faulting, and associated magmatism in Bransfield Strait, Antarctic Peninsula, *J. Geophys. Res.*, *103*, 24,017–24,043, 1998.

Barker, P. F., The Cenozoic subduction history of the Pacific margin of the

Antarctic Peninsula: Ridge crest-trench interactions, *J. Geol. Soc. London*, *139*, 787–801, 1982.

Barker, P. F., and I. W. D. Barker, Progress in geodynamics in the Scotia Arc region, in *Geodynamics in the Eastern Pacific Region, Caribbean and Scotia Arcs*, *Geodyn. Ser.*, vol. 9, edited by R. Cabré, pp. 137–170, AGU, Washington, D. C., 1983.

Barker, P. F., and I. A. Hill, Back-arc extension in the Scotia Sea, *Philos. Trans. R. Soc. London*, *300*, 249–262, 1981.

Ben Othman, D., W. M. White, and J. Patchett, The geochemistry of marine sediments, island arc magma genesis, and crust-mantle recycling, *Earth Planet. Sci. Lett.*, *94*, 1–21, 1989.

Birkenmajer, K., Age of the Penguin Island volcano, South Shetland Islands (West Antarctica), by the lichenometric method, *Bull. Pol. Acad. Sci. Earth Sci.*, *27*, 69–76, 1980.

Birkenmajer, K., Volcanic succession at Deception Island, West Antarctica: A revised lithostratigraphic standard, *Stud. Geol. Polonica*, *101*, 27–82, 1992.

Birkenmajer, K., and R. A. Keller, Pleistocene age of the Melville Peak volcano, King George Island, West Antarctica, by K-Ar dating, *Bull. Pol. Acad. Sci. Earth Sci.*, *38*, 17–24, 1990.

Cohen, R. S., and R. K. O'Nions, Identification of recycled continental material in the mantle from Sr, Nd and Pb isotopic investigations, *Earth Planet. Sci. Lett.*, *61*, 73–84, 1982.

Cousens, B. L., and J. F. Allan, A Pb, Sr, and Nd isotopic study of basaltic rocks from the Sea of Japan, ODP Leg 127/128, *Proc. Ocean Drill. Program Sci. Results*, *127/128*, 805–817, 1992.

Cousens, B. L., J. F. Allan, and M. P. Gorton, Subduction-modified pelagic sediments as the enriched component in back-arc basalts from the Japan Sea: Ocean Drilling Program Sites 797 and 794, *Contrib. Mineral. Petrol.*, *117*, 421–434, 1994.

Fisk, M. R., Volcanism in the Bransfield Strait, Antarctica, *J. South Am. Earth Sci.*, *3*, 91–101, 1990.

Forsythe, L. M., and M. R. Fisk, Comparison of experimentally crystallized and natural spinels from Leg 135, *Proc. Ocean Drill. Program Sci. Results*, *135*, 585–594, 1994.

González-Ferrán, O., The Bransfield rift and its active volcanism, in *Geological Evolution of Antarctica*, edited by M. R. A. Thomson, J. A. Crame, and J. W. Thomson, pp. 505–509, Cambridge Univ. Press, New York, 1991.

Gracia, E., M. Canals, M. Farran, M. J. Prieto, and J. Sorribas, Morphostructure and evolution of the Central and Eastern Bransfield Basins (NW Antarctic Peninsula), *Mar. Geophys. Res.*, *18*, 429–448, 1996.

Grad, M., A. Guterch, and T. Janik, Seismic structure of the lithosphere across the zone of subducted Drake plate under the Antarctic plate, West Antarctica, *Geophys. J. Int.*, *115*, 586–600, 1993.

Grad, M., A. Guterch, T. Janik, and P. Sroda, Seismic characteristic of the crust in the transition zone from the Pacific Ocean to Antarctic Peninsula, between Elephant Island and Marguerite Bay, West Antarctica, paper presented at 8th International Symposium on Antarctic Earth Sciences, R. Soc. of N. Z., Wellington, New Zealand, 1999.

Hart, S. R., J. Blusztajn, and C. Craddock, Cenozoic volcanism in Antarctica: Jones Mountains and Peter I Island, *Geochim. Cosmochim. Acta*, *59*, 3379–3388, 1995.

Hawkins, J. W., Evolution of the Lau Basin—Insights from ODP Leg 135, in *Active Margins and Marginal Basins of the Western Pacific*, *Geophys. Monogr. Ser.*, vol. 88, edited by B. Taylor and J. Natland, pp. 125–173, AGU, Washington, D. C., 1995.

Hawkins, J. W., P. F. Lonsdale, J. D. Macdougall, and A. M. Volpe, Petrology of the axial ridge of the Mariana Trough backarc spreading center, *Earth Planet. Sci. Lett.*, *100*, 226–250, 1990.

Hergt, J. M., and K. N. Farley, Major, trace element, and isotope (Pb, Sr, and Nd) variations in Site 834 basalts: Implications for the initiation of backarc opening, *Proc. Ocean Drill. Program Sci. Results*, *135*, 471–486, 1994.

Hergt, J. M., and C. J. Hawkesworth, The Pb, Sr, and Nd isotopic evolution of the Lau Basin: implications for mantle dynamics during backarc opening, *Proc. Ocean Drill. Program Sci. Results*, *135*, 505–518, 1994.

Hochstaedter, A. G., J. B. Gill, and J. D. Morris, Volcanism in the Sumisu Rift, II, Subduction and non-subduction related components, *Earth Planet. Sci. Lett.*, *100*, 195–209, 1990.

Hole, M. J., Geochemical evolution of Pliocene-Recent post-subduction alkalic basalts from Seal Nunataks, Antarctic Peninsula, *J. Volcanol. Geotherm. Res.*, *40*, 149–167, 1990.

Hole, M. J., P. D. Kempton, and I. L. Millar, The isotopic and trace element composition of small-degree melts of the asthenosphere: Evidence from the alkalic basalts of the Antarctic Peninsula, *Chem. Geol.*, *109*, 51–68, 1993.

Keller, R. A., and M. R. Fisk, Rifting and volcanism in the Bransfield Strait and South Shetland Islands, *Antarct. J. U. S.*, *23*, 102–104, 1989.

Keller, R. A., and M. R. Fisk, Quaternary marginal basin volcanism in the Bransfield Strait as a modern analogue of the southern Chilean ophiolites, in *Ophiolites and Their Modern Oceanic Analogues*, edited by L. M. Parson, B. J. Murton, and P. Browning, *Geol. Soc. Spec. Publ.*, *60*, 155–170, 1992.

Keller, R. A., M. R. Fisk, W. M. White, and K. Birkenmajer, Isotopic and trace element constraints on mixing and melting models of marginal basin volcanism, Bransfield Strait, Antarctica, *Earth Planet. Sci. Lett.*, *111*, 287–303, 1992.

Keller, R. A., J. A. Strelin, L. A. Lawver, and M. R. Fisk, Dredging young volcanic rocks in Bransfield Strait, *Antarct. J. U. S.*, *29*, 100–102, 1994.

Klepeis, K. A., and L. A. Lawver, Bathymetry of the Bransfield Strait, southeastern Shackleton Fracture Zone and South Shetland Trench, *Antarct. J. U. S.*, *28*, 103–104, 1994.

Lawver, L. A., and J. W. Hawkins, Diffuse magnetic anomalies in marginal basins: Their possible tectonic and petrologic significance, *Tectonophysics*, *45*, 323–338, 1978.

Lawver, L. A., R. A. Keller, M. R. Fisk, and J. A. Strelin, Bransfield Strait, Antarctic Peninsula: Active extension behind a dead arc, in *Back-Arc Basins: Tectonics and Magmatism*, edited by B. Taylor, pp. 315–342, Plenum, New York, 1995.

Lawver, L. A., B. J. Sloan, D. H. N. Barker, M. Ghidella, R. P. von Herzen, R. A. Keller, G. P. Klinkhammer, and C. S. Chin, Distributed active extension in Bransfield Basin, Antarctic Peninsula: Evidence from multibeam bathymetry, *GSA Today*, *6*(11), 1–6, 1996.

Leat, P. T., R. A. Livermore, I. L. Millar, and J. A. Pearce, Magma supply in back-arc spreading centre segment E2, East Scotia Ridge, *J. Petrol.*, *41*, 845–866, 2000.

Maldonado, A., and R. A. Livermore, Tectonic expression of extinct spreading centers and ridge-transform intersections in the Drake Passage (Antarctica), paper presented at 8th International Symposium on Antarctic Earth Sciences, R. Soc. of N. Z., Wellington, New Zealand, 1999.

Maldonado, A., R. D. Larter, and F. Aldaya, Forearc tectonic evolution of the South Shetland margin, Antarctic Peninsula, *Tectonics*, *13*, 1345–1370, 1994.

Marti, J., J. Vila, and J. Rey, Deception Island (Bransfield Strait, Antarctica): An example of a volcanic caldera developed by extensional tectonics, in *Volcano Instability on the Earth and Other Planets*, edited by W. J. McGuire, A. P. Jones, and J. Neuberg, *Geol. Soc. Spec. Publ.*, *110*, 253–265, 1996.

Pearce, J. A., and I. J. Parkinson, Trace element models for mantle melting: application to volcanic arc petrogenesis, in *Magmatic Processes and Plate Tectonics*, edited by H. M. Prichard et al., *Geol. Soc. Spec. Publ.*, *76*, 373–403, 1993.

Pearce, J. A., M. Ernewein, S. H. Bloomer, L. M. Parson, B. J. Murton, and L. E. Johnson, Geochemistry of Lau Basin volcanic rocks: Influence of ridge segmentation and arc proximity, in *Volcanism Associated With Extension at Consuming Plate Margins*, edited by J. L. Smellie, *Geol. Soc. Spec. Publ.*, *81*, 53–75, 1995.

Pelayo, A. M., and D. A. Wiens, Seismotectonics and relative plate motions in the Scotia Sea region, *J. Geophys. Res.*, *94*, 7293–7320, 1989.

Pouclet, A., J.-S. Lee, P. Vidal, B. Cousens, and H. Bellon, Cretaceous to Cenozoic volcanism in South Korea and in the Sea of Japan: magmatic constraints on the opening of the back-arc basin, in *Volcanism Associated With Extension at Consuming Plate Margins*, edited by J. L. Smellie, *Geol. Soc. Spec. Publ.*, *81*, 169–191, 1995.

Rocholl, A., M. Stein, M. Molzahn, S. R. Hart, and G. Worner, Geochemical evolution of rift magmas by progressive tapping of a stratified mantle source beneath the Ross Sea Rift, Northern Victoria Land, Antarctica, *Earth Planet. Sci. Lett.*, *131*, 207–224, 1995.

Saunders, A. D., Geochemistry of basalts recovered from the Gulf of California during Leg 65 of the Deep Sea Drilling Project, *Initial Rep. Deep Sea Drill. Proj.*, *65*, 591–621, 1983.

Saunders, A. D., and J. Tarney, The geochemistry of basalts from a back-arc spreading centre in the East Scotia Sea, *Geochim. Cosmochim. Acta*, *43*, 555–572, 1979.

Saunders, A. D., and J. Tarney, Geochemical characteristics of basaltic volcanism within back-arc basins, in *Marginal Basin Geology: Volcanic and Associated Sedimentary and Tectonic Processes in Modern and Ancient Marginal Basins*, edited by B. P. Kokelaar and M. F. Howells, *Geol. Soc. Spec. Publ.*, 16, 59–76, 1984.

Saunders, A. D., D. J. Fornari, and M. A. Morrison, The composition and emplacement of basaltic magmas produced during the development of continent-margin basins: The Gulf of California, Mexico, *J. Geol. Soc. London*, *139*, 335–346, 1982.

Smellie, J. L., Lithostratigraphy and volcanic evolution of Deception Island, South Shetland Islands, *Antarct. Sci.*, *13*, 188–209, 2001.

Smellie, J. L., R. J. Pankhurst, M. R. A. Thomson, and R. E. S. Davies, The geology of the South Shetland Islands, VI, Stratigraphy, geochemistry and evolution, *Br. Antarct. Surv. Sci. Rep.*, *87*, 85 pp., 1984.

Smellie, J. L., A. Hofstetter, and G. Troll, Fluorine and boron geochemistry of an ensialic marginal basin volcano: Deception Island, Bransfield Strait, Antarctica, *J. Volcanol. Geotherm. Res.*, *49*, 255–267, 1992.
Smellie, J. L., P. Stone, and J. Evans, Petrogenesis of boninites in the Ordovician Ballantrae Complex ophiolite, southwestern Scotland, *J. Volcanol. Geotherm. Res.*, *69*, 323–342, 1995.
Stern, R. J., P.-N. Lin, J. D. Morris, M. C. Jackson, P. Fryer, S. H. Bloomer, and E. Ito, Enriched back-arc basin basalts from the northern Mariana Trough: Implications for the magmatic evolution of back-arc basins, *Earth Planet. Sci. Lett.*, *100*, 210–225, 1990.
Stolper, E., and S. Newman, The role of water in the petrogenesis of Mariana Trough magmas, *Earth Planet. Sci. Lett.*, *121*, 293–325, 1994.
Sun, S.-S., and W. F. McDonough, Chemical and isotopic systematics of oceanic basalts: implications for mantle composition and processes, in *Magmatism in the Ocean Basins*, edited by A. D. Saunders and M. J. Norry, *Geol. Soc. Spec. Publ.*, *42*, 313–345, 1989.
Tamaki, K., K. Suyehiro, J. Allan, J. C. Ingle, and K. A. Pisciotto, Tectonic synthesis and implications of Japan Sea ODP drilling, *Proc. Ocean Drill. Program Sci. Results*, *127/128*, Part 2, 1333–1348, 1992.
Tatsumi, Y., D. L. Hamilton, and R. W. Nesbitt, Chemical characteristics of fluid phase released from a subducted lithosphere and origin of arc magmas: Evidence from high-pressure experiments and natural rocks, *J. Volcanol. Geotherm. Res.*, *29*, 293–309, 1986.
Taylor, B., and G. D. Karner, On the evolution of marginal basins, *Rev. Geophys.*, *21*, 1727–1741, 1983.
Taylor, B., G. Brown, P. Fryer, J. B. Gill, A. G. Hochstaedter, H. Hotta, C. H. Langmuir, M. Leinen, A. Nishimura, and T. Urabe, *Alvin*-SeaBeam studies of the Sumisu Rift, Izu-Bonin arc, *Earth Planet. Sci. Lett.*, *100*, 127–147, 1990.
Volpe, A. M., J. D. Macdougall, and J. W. Hawkins, Lau basin basalts (LBB): Trace element and Sr-Nd isotopic evidence for heterogeneity in backarc basin mantle, *Earth Planet. Sci. Lett.*, *90*, 174–186, 1988.
Volpe, A. M., J. D. Macdougall, G. W. Lugmair, J. W. Hawkins, and P. F. Lonsdale, Fine-scale isotopic variation in Mariana Trough basalts: Evidence for heterogeneity and a recycled component in backarc basin mantle, *Earth Planet. Sci. Lett.*, *100*, 251–264, 1990.
Weaver, S. D., A. D. Saunders, R. J. Pankhurst, and J. Tarney, A geochemical study of magmatism associated with the initial stages of back-arc spreading: The Quaternary volcanics of Bransfield Strait, from South Shetland Islands, *Contrib. Mineral. Petrol.*, *68*, 151–169, 1979.
White, W. M., M. M. Cheatham, and R. A. Duncan, Isotope geochemistry of Leg 115 basalts and inferences on the history of the Reunion mantle plume, *Proc. Ocean Drilling Program Sci. Results*, *115*, 53–61, 1990.

M. R. Fisk and R. A. Keller, College of Oceanic and Atmospheric Sciences, Oregon State University, 104 Ocean Admin Bldg., Corvallis, OR 97331, USA. (mfisk@coas.oregonstate.edu; rkeller@coas.oregonstate.edu)

L. A. Lawver, Institute for Geophysics, University of Texas at Austin, 4412 Spicewood Springs Road #600, Austin, TX 78759, USA. (lawver@ig.utexas.edu)

J. L. Smellie, British Antarctic Survey, High Cross, Madingley Road, Cambridge CB3 0ET, UK. (jlsm@bas.ac.uk)

J. A. Strelin, Instituto Antartico Argentino, CADIC-CONICET-Malvinas Argentinas S/No, 9410 Ushuaia, Argentina. (jstrelin@satlink.com)